CHEMICAL MECHANICAL POLISHING OF COPPER USING NANOPARTICLE-BASED SLURRIES

By

SU-HO JUNG

A DISSERTATION PRESENTED TO THE GRADUATE SCHOOL
OF THE UNIVERSITY OF FLORIDA IN PARTIAL FULFILLMENT
OF THE REQUIREMENTS FOR THE DEGREE OF
DOCTOR OF PHILOSOPHY

UNIVERSITY OF FLORIDA

2005

This study is dedicated to my family.

ACKNOWLEDGMENTS

I would like to sincerely appreciate my advisor, Dr. Rajiv Singh, for his guidance and support throughout this study. Not only his financial support helped me pursue this research work but also his sincere dedication and great enthusiasm to advance this research area have inspired this research much. I also would like to acknowledge Dr. Brij Moudgil and Dr. Chang-Won Park for their constant and valuable discussions, during the weekly CMP meetings. I also would like to acknowledge the members of my advisory committee, Dr. Hassan El-Shall, Dr. Stephen Pearton, and Dr. Dinesh Shah, for their consideration and time to discuss this research.

I would like to acknowledge the National Science Foundation/Particle Engineering Research Center for financial support of part of this research. I also would like to acknowledge staff members of Particle Engineering Research Center, Materials Analytical Instrumentation Center, and the Department of Materials Science and Engineering: Wayne Acree, Edward Bailey, Mike Beasly, Jerry Bourne, Gill Brubaker, Valentin Craciun, Luisa Amelia Dempere, Anne Donnelly, Doris Harlow, John Henderson, Jennifer Horton, Eric Lambers, Sophie Leone, Martha McDonald, Gary Scheiffele, Kerry Sieben, Jo-Ann Standridge, and Mike Tollon, who helped me much in this research. Special thanks go to our secretary, Margaret Rathfon, who took care of me like my family does, especially in a situation in which I was far away from my family across a huge ocean.

Many thanks go to my old and present colleagues Jeremiah Abiade, Bahar Basim, Nabil Bassim, Scott Brown, Kyoung-Ho Bu, Jaeyoung Choi, Won-Seop Choi, Madhavan Esaynaur, Chad Essary, Josh Howard, Frank Kelly, Won-Seok Kim, Vishal Kosla, Seung-Mahn Lee, Mike Ollinger, Karthik Ramani, Danielle Stodilka, Suresh Yeruva, and Sang Yoon, who not only helped and encouraged me in this research but also made my graduate study years lots of fun.

Finally I would like to thank my family members: my parents, Ok-Suk Jung and Hee-Jin Jung, who have given me this enormous love that made this thesis possible, and my sister, Su-Yeoun Jung, and her husband, Kyung-Hwan Kim, who have constantly cheered me with their support.

TABLE OF CONTENTS

page

LIST OF TABLES

LIST OF FIGURES

Abstract of Dissertation Presented to the Graduate School
of the University of Florida in Partial Fulfillment of the
Requirements for the Degree of Doctor of Philosophy

CHEMICAL MECHANICAL POLISHING OF COPPER USING NANOPARTICLE BASED SLURRIES

By

Su-Ho Jung

May 2005

Chair: Rajiv K. Singh
Major Department: Materials Science and Engineering

Chemical mechanical polishing (CMP) is a vital step for planarizing multi-level interconnect structures in ultra large-scale integrated circuit applications. The CMP has become the fastest growing semiconductor manufacturing operation in the past decade and is expected to continue its high growth rate with the emergence of next generation interconnect materials such as copper and ultra-low dielectric constant insulators in the coming decade. However, these next generation interconnects, due to their fragility and poor adhesion, are susceptible to CMP-induced defect formation such as microscratches, copper and barrier peeling, low k damage, dishing, and erosion. The state-of-the-art slurries presently designed for polishing copper/silica dielectric use hard aggregate particles (fumed alumina, 100-300 nm in diameter), which, we believe, may not be easily extended to polishing of copper/low k or ultra low k dielectrics.

In this study, we investigate copper CMP using nanoparticle based slurries to reduce the defect formation. The reduction of defect formation, however, is among other

considerations such as high removal rate. We examine the nanoscale synergistic chemical and mechanical interactions to determine controlling factors in defectivity and removal rate. Our experimental results indicate that the synergistic effect, that is, the rapid formation of surface passive layer that can be subsequently removed by the nanoparticles without deforming underlying bare copper, is needed to obtain the 'gentle' copper CMP. The removal rate is synergistic, but more dominated by the chemical reaction than by the mechanical abrasion. The formation mechanism of the removable surface layer is investigated. It is suggested that the enhanced the reaction kinetics of the layer formation by addition of chelating agent in the slurry leads to a less dense oxide layer on copper surface that can be removed by the nanoparticles. The role of nanoparticle size and concentration is also studied to understand in what manner the material removal occurs. The results show that the indentation volume of the particle onto the surface layer plays an important role in material removal.

CHAPTER 1
INTRODUCTION

The constant device miniaturization driven by semiconductor industry in the last decade has required advanced interconnect schemes. As the device gets smaller and smaller, the delay of interconnects that wire the transistors non-linearly increases, whereas the delay of gates that switch the transistors significantly decreases. Below a micrometer feature size, the interconnect delay measured by RC (resistance x capacitance) of a circuit is much larger than the gate delay and becomes a rate limiting factor for the total device speed.

To reduce the interconnect delay, new multilevel interconnect (MLI) schemes, which span several planes, have been developed. To further reduce the interconnect delay, the conventional interconnect materials such as aluminum (metal) and silica (dielectric) can be replaced by low resistivity metal such as copper and low dielectric insulating materials such as fluorinated silica, carbon-doped silica, and polymers. By integrating copper and the low k dielectrics, the MLI structure can provide (i) significant reduction in interconnect delay that leads to increased device speed (ii) enhanced electromigration resistance, and (iii) reduced number of layers.

Due to the lack of dry gas phase etching chemistries for copper, however, chemical mechanical polishing (CMP) is the only method for nanomachining the copper-based MLI. The method known as ‘damascene’ is utilized to fabricate the copper-based MLI, which deposits excess amount of copper on dielectric patterned with trenches and then

employs the CMP step to rapidly remove the overburden copper and globally planarize the structure.

The advent of copper and the low k dielectrics as interconnect materials has indeed accelerated the need of CMP process but also introduced a new set of challenges. These next generation interconnect materials are quite fragile and exhibit poor adhesion property and thus are very susceptible to CMP induced normal and shear stresses. It is also noted that mechanical strengths of dielectric films significantly decrease with a decrease of dielectric constants of the films. Consequently the defect formation such as microscratches, copper-barrier peeling, low k damage, dishing, erosion, and so on have been often observed during the CMP process. Such defect formations not only negatively impact the successive process loop but also are ultimately detrimental to the device performance [Sin03, Wan01], which however still remains as one of the biggest challenges of the CMP for copper and low k dielectric integration.

To reduce the defect formation, various investigations such as reduction in down pressure [Kon03], abrasive-free polishing [Pad03], electro-polishing [Cha03], and so on have been conducted. The challenging aspects of these approaches towards the ‘gentle’ copper CMP, however, appeared to be balancing with other demanding output parameters such as removal rate and planarity. This is primarily because these approaches are based on the cause-and-effect relationship and are lack of thorough understanding of the time-dependent wafer-slurry-pad interactions that are complicated by the large number of slurry variables and their synergistic effects.

To mitigate these challenges, we have earlier proposed a mechanistic methodology of understanding the wafer-pad-slurry interactions, namely micro- and nano-scale interactions [Sin02].

Mechanical stresses during the CMP process can be related to particle indentation (penetration) into the wafer surface. According to the contact mechanics theory [Zha02, Qin04], the particle indentation during the CMP process may depend upon (i) particle properties, (ii) properties of chemically modified surface layer, and (iii) pad modulus. Hardness and size of the particle can be reduced to lower the penetration, thus avoiding the damaging effects. The state-of-the-art slurries presently designed for polishing copper/silica use hard aggregate particles (fumed alumina, 100-300 nm in diameter). We believe that this may not be easily extended to polishing of copper/low k or ultra low k dielectrics.

This thesis describes an investigation into the chemical mechanical polishing of copper using sub 100 nm silica particles. The objective of this work is to examine synergistic chemical-mechanical effects during the copper CMP process. The influence of synergistic interactions on polishing characteristics (or polishing output parameters) such as defectivity and removal rate, and the role of each individual component, chemical and mechanical, in the synergy are studied throughout. In chapter 2, more details of current understanding are reviewed. The experimental procedures used in this thesis are described in chapter 3. In chapter 4, synergistic chemical-mechanical effects on controlling the defect formation and removal rate are examined. This chapter also compares and contrasts the results obtained by the nanoparticles with the results obtained by two other types of particles, one micron-size silica and 200 nm alumina particles. In

chapter 5, the formation mechanism of a surface passive layer that can be removed by the nanoparticles is investigated. In chapter 6, the removal mechanism by studying the role of nanoparticle size and concentration is investigated. The conclusions is given in chapter 7.

CHAPTER 2
LITERATURE REVIEW

Chemical mechanical polishing (CMP) is a technique that removes excess material and planarizes an uneven surface. Although adopted by semiconductor industry for silicon wafer polishing around 40 years ago, the technique has long been used to obtain a mirror surface. In the last decade, the CMP process has become a vital step for fabricating microelectronic devices in ultra large-scale integrated circuit (ULSI) applications, such as shallow trench isolation (STI) and multi-level interconnects (MLI). This enabling process to significantly reduce topographical variation and to provide excellent surface finish is also rapidly stretching to other numerous applications such as micro-electro mechanical systems (MEMS), compound semiconductors, and ferro-electric and –magnetic random access memories (FeRAM).

Need of Chemical Mechanical Polishing

Rapid advances in ultra large-scale integrated circuits (ULSI) for miniaturized chip size and improved performance have raised demand for enhanced metallization schemes.

Multilevel Interconnect and Damascene

Fig. 1 illustrates the schematic of interconnect that includes metal lines, insulator and substrate. The delay of interconnect is represented by RC (resistance x capacitance) of the circuit components. By taking into account the metal resistance and capacitances (metal-metal and metal-substrate), the total RC delay can be expressed as following,

$$RC \propto \rho\varepsilon\varepsilon_0 L^2\left(\frac{1}{wd}+\frac{1}{t_M t_D}\right) \qquad (2.1)$$

With decrease in the feature size (< 0.25 μm), the first term in the parenthesis ($1/wd$) becomes dominant. The RC delay of a circuit increases non-linearly and is much larger than the delay in switching the transistor (gate delay) [Rya95]. To reduce the RC time delay, new multilevel interconnect (MLI) schemes, which span several planes and are isolated by dielectric insulating layers, have been developed. To further reduce the RC delay, low resistivity (ρ) materials such as copper (alternative for aluminum) and low dielectric constant (ε) materials such as fluorinated silica, carbon-doped silica and polymers (alternative for silicon dioxide) can be used [Sho00]. Therefore, the MLI scheme based on Cu/low-K promises significant improvements in operating the miniaturized devices.

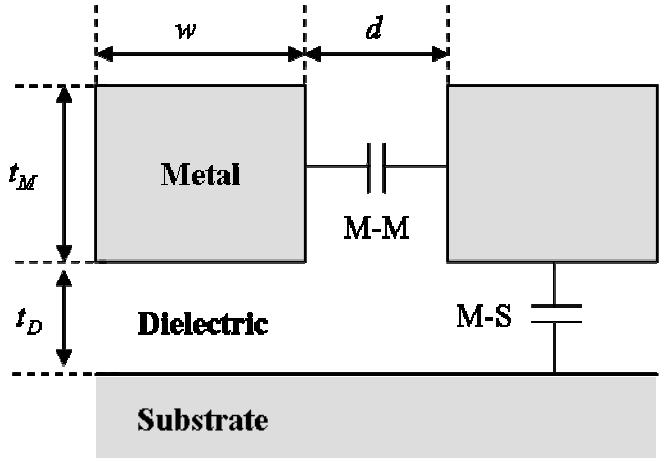

Figure 2-1 Schematic of the interconnect that shows metal lines and insulating dielectrics

Due to the lack of dry gas phase etching chemistries for copper, chemical mechanical polishing (CMP) has been almost the sole method to achieve planarization of

copper and eventually to build the MLI structure. This method known as the damascene process deposits blanket metal on dielectric which has been patterned with trenches and then employs CMP to polish the top continuous overburden metal layer [Mur00]. To make very thin copper lines, the following steps are conducted: (i) deposition of low k dielectric (or silica) layer, (ii) patterning of the silica (or low k dielectric layer) by dry gas phase etching, (iii) deposition of a thin Ta (or TaN layer) which acts as an adhesion layer and also a diffusion barrier, (iv) deposition of a thin copper layer as seed layer by physical vapor deposition, (v) thick copper deposition by electroplating, and (vi) chemical mechanical polishing to remove the overburden regions so that nanoscale copper lines are exposed (Fig. 2-3).

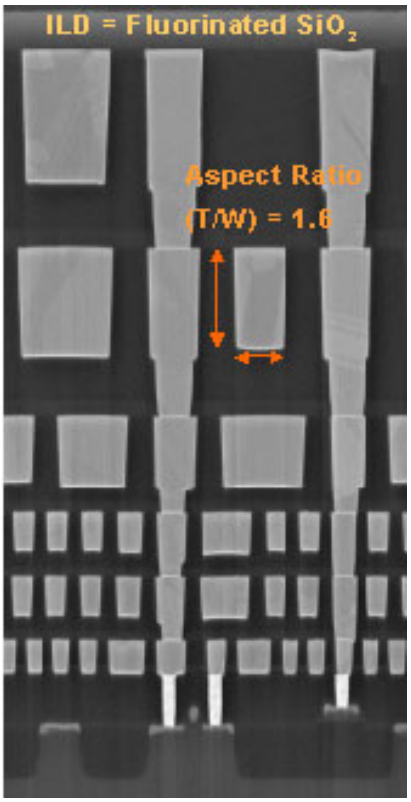

Figure 2-2 Multi-level interconnect (MLI) structure integrated with copper and low k dielectrics (fluorinated SiO2) [Intel].

Challenges in Integrating Copper and Low k Dielectrics

The next generation interconnect materials such as copper and low k dielectrics, due to their fragility and poor adhesion, are susceptible to CMP-induced contact stresses (normal and shear) and defect formation such as microscratches, copper and barrier layer delamination, low k damage, dishing, and erosion [Sin03, Wan01].

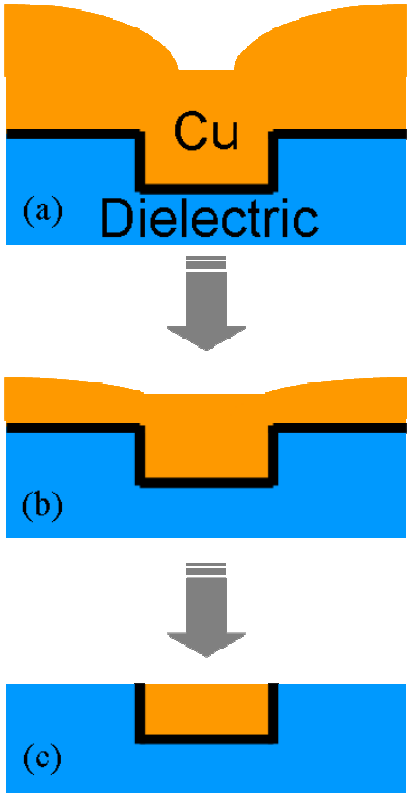

Figure 2-3. Flow chart of interconnect fabrication by damascene process (a) copper is deposited after the insulating dielectric is patterned with a trench (b) overburden copper is removed with CMP process (c) planarized single interconnect layer. These processes are repeated to build the MLI structure.

Principle of Chemical Mechanical Polishing

The CMP Process

A schematic diagram of the CMP process is shown in Fig. 2-4. A typical rotary CMP tool consists of a polishing pad affixed to a circular polishing plate, a carrier to hold a wafer against the pad, and slurry. Both the carrier and the plate are rotated as the front of the wafer is pressed down against the pad, which is covered with the polishing slurry. The polishing slurry provides the means by which both chemical and mechanical (tribological) actions are used to remove and subsequently planarize the wafer surface. A typical CMP process mainly consists of three components; wafer, slurry, and pad. As illustrated in Fig. 2-4, the wafer is pressed against the pad with a normal force and moves along the spinning pad with a relative velocity. The polishing slurry that contains chemical additives and abrasive particles is fed onto the pad and travels between the pad and the wafer surface. The pad is normally made of porous polymer (polyurethane) and has several functions: (i) uniform slurry transport and distribution, (ii) removal of reacted products (debris, etc.), and (iii) uniform pressure distribution across the wafer.

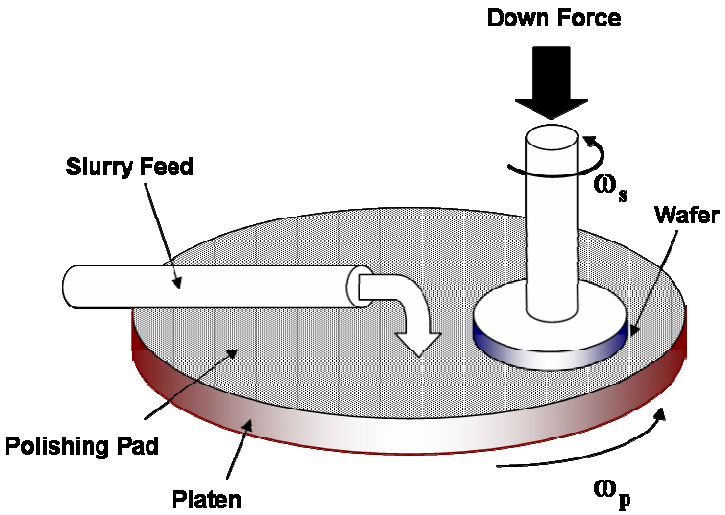

Figure 2-4 Schematic of typical CMP apparatus that includes wafer, pad, and slurry.

The performance of CMP may be categorized as removal rate, planarization, defectivity, and selectivity. Removal rate is related to throughput issue of the process. For industrial perspective, fast removal rate is needed for mass production of wafers, which is usually estimated 400-600 nm/min for copper. The deposited overburden films on patterned surfaces have large lateral dimensions (currently 300 mm) and wide variations of pattern-dependent topography. The pitch of the pattern (the sum of the width of the patterned lines and the spacing between them) as well as its density can vary significantly across the die. The removal of such a complex structured surface requires 'global planarization.' Defect formation during the process is another issue and become quite significant when next generation interconnects such as copper/low k dielectrics are integrated. A variety of defects such as microscratches, metal-barrier layer peeling, dielectric damage, dishing, and erosion are often observed and must be minimized. Selectivity is defined as the ratio of top layer removal rate to underlying layer removal rate. In copper CMP, as seen in damascene process, the selectivity refers removal of copper vs. barrier (Ta or TaN) vs. dielectric (SiO_2 or low k dielectrics). A high selectivity value is desired because the CMP process needs to stop once the top layer is removed.

The performance quality of the CMP process is, of course, determined by optimization of the process variables including the polishing slurry. One of the unique features of the CMP is that the material removal and planarization normally take place via the synergistic interactions. These combinatorial effects that combine both chemical and mechanical effects are intuitively different from chemical dissolution-type or mechanical polishing-type of material removal. In general, the chemical agents are responsible for surface reaction, while the abrasive particles are responsible for

mechanical action. Although the tool operation itself is relatively simple, strict control and deep understanding of the process are often complicated by the exceedingly large number of process variables (> 20), their synergistic interactions, and the dynamic nature of the process.

Since metal CMP involves electrochemical origins, a Pourbaix diagram (Fig. 2-5) usually illustrates a concisely visual and rational approach to the slurry chemistry. The Pourbaix diagram is a member of a general class of thermodynamic diagrams that are termed aqueous stability or predominance area diagrams (potential vs. pH) [Pou74]. Slurries employed for planarization of metal typically include an oxidizer to form metal oxides, a corrosion inhibitor to prevent high static etch rates, and a complexing agent to enhance solubility of metals or to soften the layer. The dissolution and passivation processes resulted from the combination of these chemical additives are very competitive, and must be tunable to attain ideal planarization. Therefore, it also should be pointed out that the chemically modified surface layer with different characteristics (composition, harness, thickness) may form in various slurries depending upon thermodynamic basis, the pH and electrochemical potential of the metal in the slurry, and also kinetics of the various reactions that are thermodynamically favorable at the given pH and potential [Ste97]. The state-of-the-art slurry chemicals employed for planarization of copper typically include hydrogen peroxide as the oxidizer, benzotriazole as the corrosion inhibitor, and citric acid or glycine as the complexing agent. The dissolution and passivation processes resulted from the combination of these chemical additives are very competitive, and must be tunable to attain ideal planarization. Therefore, a chemically modified surface layer with different characteristics (composition, hardness, thickness)

may form in various slurries depending upon thermodynamic basis, the pH and electrochemical potential of the metal in the slurry, and also kinetics of the various reactions that are thermodynamically favorable at the given pH and potential [Lee03].

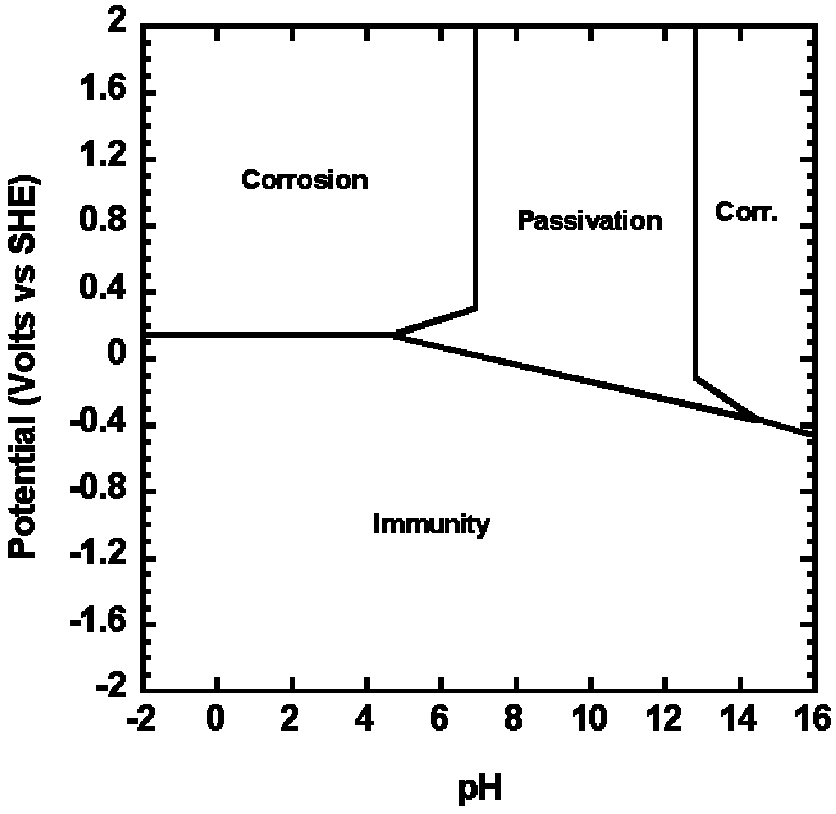

Figure 2-5 Typical Pourbaix diagram. Boundary lines indicate equilibrium between either a solid phase and an ion or two solid phases. Within the boundary, regions of corrosion, passivation, and immunity are shown [Pou74].

In conjunction with slurry chemistry, abrasives also play an important role in CMP performance such as material removal rate and surface finish. A variety of abrasive materials have been utilized in industry, which typically include commercially available Al_2O_3 and SiO_2 particles for metal CMP. A large number of characteristics are used to

determine their roles in the polishing process. The abrasives are mainly responsible for mechanical action of the slurry. Thus the most attention-grabbing issues for the semiconductor industry are their causes of surface scratching, denting, and peeling during polishing soft metal like copper [Sin03]. In addition, the large differences between the hardness of the metal and the slurry abrasive can further accentuate special type of defects known as “dishing” and “erosion” that results in non-planarity. These defects addressed are detrimental to both fabricating and operating IC devices.

Despite their importance, effects of abrasive particle on CMP performance are somewhat inconclusive. Experimental results reported are quite contradicting [Mah99, Bie98, Zho02, Bou02, Lu03], and its roles in modeling work are not experimentally proven yet [Coo90, Qin04, Zha02]. This is primarily due to limitations and difficulties of experimental approach that lead to lack of understanding the fundamental aspects of small-scale interactions that take place during the polishing. It is very difficult to precisely resolve the individual effect because (i) a large number of other input variables is introduced, (ii) the entire process is exceedingly dynamic, transient, and synergistic, and (iii) the actual removal takes place on a very small scale (Å to nm).

The CMP Mechanisms

Due to its simplicity, Preston’s law has been the most extensively used equation in describing the mechanism of CMP, which states that the removal rate of a material, that is, the thickness decrease (Δh) over time (Δt) is directly proportional to the applied pressure (P) and relative velocity (V) of the particles across the wafer [Pre27].

$$RR = \Delta h / \Delta t = K_p \cdot P \cdot V \qquad (2.2)$$

Preston's constant (K_p) depends on properties of the polishing pad, slurry, and materials to be polished. Although Preston's equation has been a basis for illustrating general polishing, it does not provide profound insight of synergistic phenomena (chemical and tribological dynamics of surface layer formation, contact mechanics, etc.) during CMP, due to its initial development for mechanical polishing of glass.

The electrochemical effect and material removal mechanism in metal CMP were first proposed by Kaufmann [Kau91]. In metal CMP, the chemical action by the slurry chemical dissolves the metal surface and forms a passivating film preventing the isotropic chemical etching process on the wafer surface. By the mechanical action of the abrasive particles and the polishing pad, the passivated film is removed, achieving a degree of global planarization that is unmatched by the chemical etching process. In general, the dissolution rate of the metal surface was found to be two orders of magnitude lower than the polishing rate [Sin02].

Singh et al. [Sin02] outlined mechanistic methodology for understanding the wafer-pad-slurry interactions during the CMP process, namely micro- and nanoscale effects. The large number of process variables with micro- and nano-scale effects and output parameters are summarized in Table 1. The micro-scale perception involves identification of polishing mode in which the particle based slurry interacts with the comparatively rough pad and the flat wafer surface. It is generally believed that the majority of material removal takes place on a contact mode, that is, the active numbers of particles that are trapped between the pad asperity and the wafer surface under certain down pressure participate mostly in material removal. It is therefore critical to be aware of the real area of wafer-pad contact, the fraction of particles that cover the pad surface (fractional

surface coverage), and so on. The nano-scale perception takes into account the formation of surface layer by chemical additives and its subsequent removal by particle abrasion, which generally occurs in nano- or atomic scale within a very short time (~ millisecond). Therefore, it is important of understand the dynamics of surface layer formation (transient characteristics) and its physical interaction with the abrasive particle such as indentation depth.

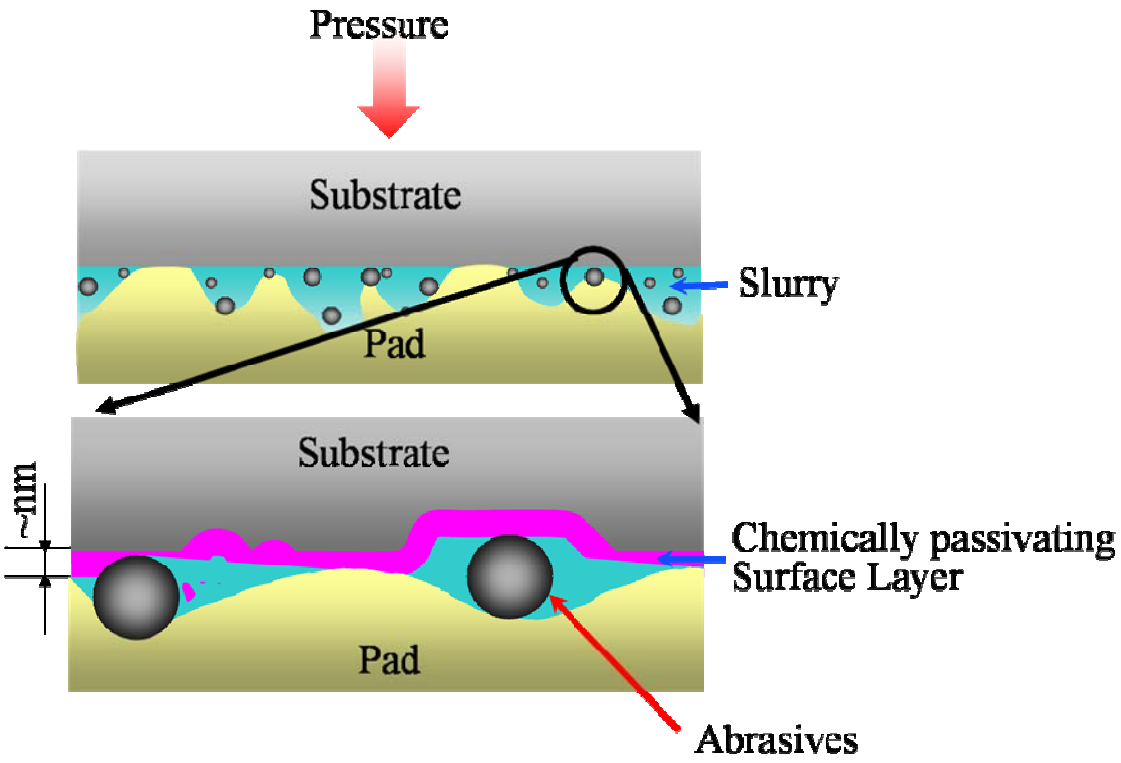

Figure 2-6 Schematic illustration of microscale and nanoscale phenomena during CMP [Sin02]

Wafer-Slurry-Pad Interactions in Micro- and Nano-Scales

Real Area of Pad-Wafer Contact

One of the distinctive features of CMP phenomena from conventional tribology is the contact of two solids, the pad and the wafer. The pad is typically made of porous

polymeric materials, which is more compliant than the oxide- or metal-wafers. The roughness of the pad can be characterized to be much higher than that of the wafer (the difference can be up to 3-4 orders of magnitude). Therefore, when the pad and the wafer are in physical contact and pressed against each other, it is generally accepted that only certain portion of the pad can be deformed on the wafer surface.

Fig. 2 illustrates the contact between a polishing pad and the wafer, first proposed by Yu et al. [Yu93]. Yu et al. statistically analyzed roughness of the polishing pad using the Greenwood-Williamson elastic model [Gre66, Gre67]. The assumptions in the model were (i) spherical shaped asperity and (ii) Gaussian distribution of variations in asperity height and radius of the sphere. Assuming the direct contact mode of polishing regime, the applied load can be carried solely by the pad asperities. The total contact area (A_{con}) and load (L) over a nominal pad area (A) was calculated as

$$A_{con} = \eta \int_{d}^{\infty} \int_{0}^{\infty} a \Phi_{\beta} \Phi_{z} d\beta dz \qquad (2.3)$$

$$L = \eta A \int_{d}^{\infty} \int_{0}^{\infty} l \Phi_{\beta} \Phi_{z} d\beta dz \qquad (2.4)$$

where η is the asperity density, β is the asperity radius, z is the asperity height, Φ_{β} and Φ_{z} are the Gaussian distribution functions of the asperity radius and the asperity height, respectively. The contact pressure is $P_{con} = L / A_{con}$. Fig. 3 shows the calculated P_{con} and A_{con} against P. As shown in the figure, the pad contact area increases with an increase of down load while the pad contact pressure is almost constant with the increase of down load due to the increase in the contact area. This result suggests that applied down pressure controls the polishing via the pad contact area rather than the pad contact

pressure. At 7 psi, A_{con}/A varies from 0.05 to 0.54 %, depending on the pad modulus (10-100 MPa).

Basim et al. [Bas03] experimentally verified this model using the Fourier transform infrared spectroscopy/attenuated total internal reflection spectroscopy (FTIR/ATR) technique. A sample pad (IC-1000) was placed on the (ZnSe) ATR crystal and loaded from 3.4 to 11.4 psi. The intensities of the CH_2 peaks of the polyurethane were recorded at wave number range 3000-2750 cm^{-1} by measuring the area under the detected peak. As shown in Fig. 4a, five spectra were collected at each pressure level. The percent pad contact area was then determined by comparing these intensity values with the value of a 100 % pad contact with non-porous, defect-free and flat surface. The real contact area of the pad (IC-1000, E=30-40 MPa [Oer85, Tic99]) was experimentally estimated as 0.33 % at 7 psi which is in good agreement with the Yu's calculated result.

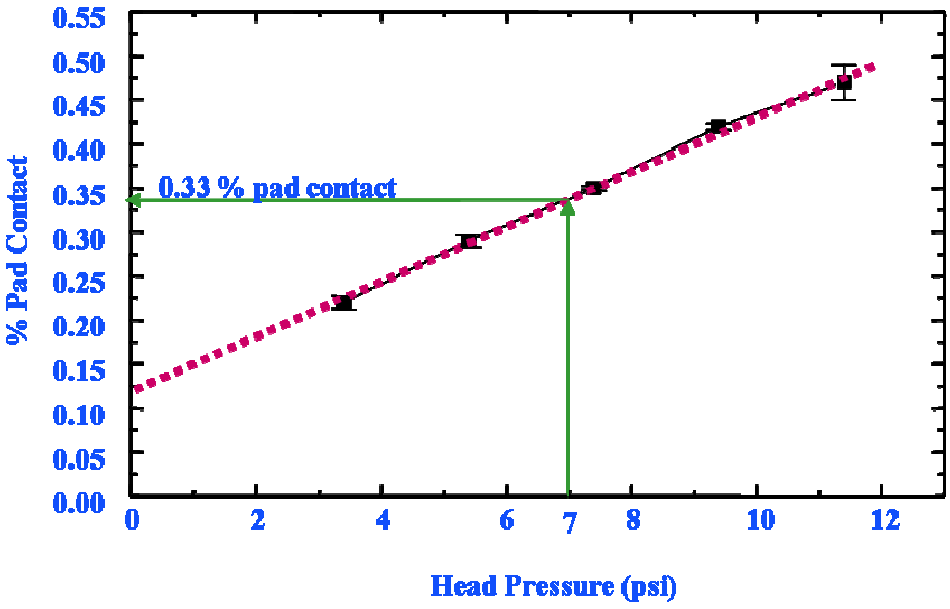

Figure 2-7 Percent pad (IC 1000) contact area on wafer surface as a function of applied load obtained by FRIR/ATR technique [Bas03].

Fractional Surface Coverage

As we assume in this work that the majority of material removal takes place on the direct contact mode, the number of particles placed at the real area of the pad-wafer contact should be understood.

Cook and Brown et al. [Bro81, Coo90] described the fractional surface coverage of particles during polishing using the concept of particle fill fraction (*K*) on the entire wafer surface. The model was premised on the flat and hard pad surface without asperity. Then the number of particles per unit area can be expressed by the following:

$$N / A = \frac{2K}{\sqrt{3}\phi^2} \qquad (2.5)$$

K is unity for fully hexagonal close packing. The force per single particle when trapped between two hard surfaces can be expressed as follows:

$$F_\phi = \frac{\sqrt{3}P\phi^2}{2K} \qquad (2.6)$$

where *P* is the polishing pressure, ϕ is the diameter of particle, and F_ϕ is the force per individual particle.

Choi et al. [Cho04] used in situ friction force measurements to estimate fractional surface coverage. To estimate the real number of particle-pad contact, experiments were conducted with relatively soft silica abrasive particle (Vicker's hardness = 540 kg/mm^2) and hard sapphire wafer (2370 kg/mm^2). The fractional surface coverage that is actually in contact with both the pad asperity and the wafer surface is calculated by measuring the in situ friction force. According to the Amonton's law, friction force (F) is defined as product of the friction coefficient (μ) and normal force (F_N).

$$F = \mu F_N \qquad (2.7)$$

The normal force can be written as follows:

$$F_N = PA \tag{2.8}$$

Combining Eq. (5) and (6), friction force can be determined by following relationship,

$$F = \mu PA \tag{2.9}$$

Total F equals the sum of the friction force due to the particles and the wafer surface (F_ϕ) and the friction force due to the pad and the wafer surface (F_p):

$$F = F_\phi + F_p = \mu_\phi P_\phi A_\phi + \mu_p P_p A_p \tag{2.10}$$

Since the typical CMP pads are compliant, it may be assume that the real contact pressure (P_{con}) remains unchanged ($P_{con}=P_\phi=P_p$):

$$F = P_{con}\left(\mu_\phi A_\phi + \mu_p A_p\right) = A_{con} P_{con}\left(f_\phi \cdot \mu_\phi + (1 - f_\phi)\mu_p\right) \tag{2.11}$$

where A_{con} is the real contact area and f is the fractional surface coverage (A_ϕ/A_{con}). Then an equation for fractional surface coverage for CMP with soft pads can be established:

$$f_\phi = (F - \mu_p P_{con} A_{con}) / (\mu_\phi P_{con} A_{con} - \mu_p P_{con} A_{con}) \tag{2.12}$$

The experimental results showed that the fractional surface coverage of particles is independent of down load and increases with solids loading. The decrease of particle size leads to an increase in the total contact area of particles in contact with wafer, leading to a higher fraction of slurry particles in contact with the wafer.

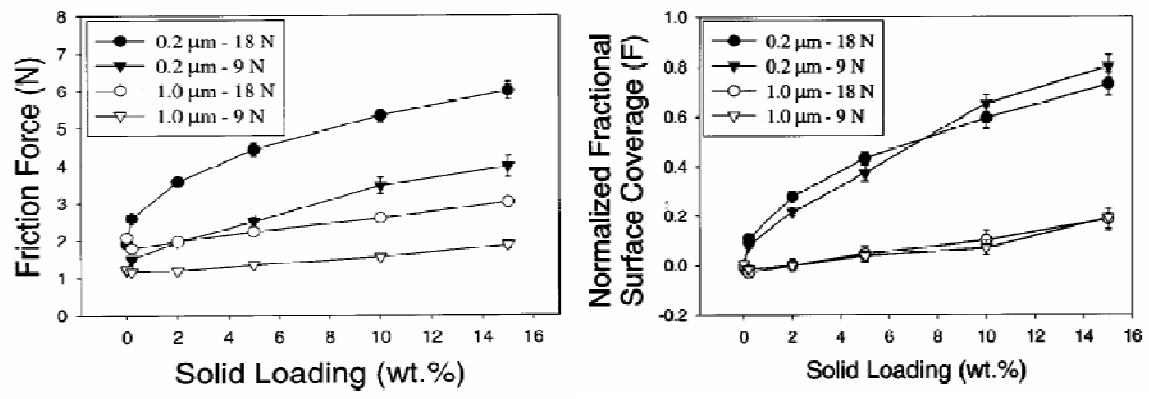

(a) (b)

Figure 2-8 Estimation of fractional surface coverage using in situ friction force measurements [Cho04] (a) in situ friction force as a function of solids loading for different down pressure and particle size (b) normalized fractional surface coverage of particles in contact with wafer surface, converted from (a).

Formation of Chemically Modified Surface Layer

It is well established that the slurry chemistry significantly influences copper surface properties such as dissolution and passiviation. These parameters are integral for controlling the properties and kinetics of chemically modified surface layer formation and therefore will ultimately influence polishing characteristics such as removal rate, planarity, surface quality, and defectivity. Polishing slurries for copper CMP typically contain the following [Tam02]:

1. Oxidizer to form a surface oxide layer,
2. Corrosion inhibitor to prevent dissolution of copper,
3. Chelating agent to increase the copper removal rate.

Earlier investigations on copper CMP largely utilized tools that were used for corrosion-related studies. Traditional methods of measuring corrosion effects such as potentiodynamic scans, and a.c. impedance provide important information on the

dissolution/passivation behavior but, due to the dynamic nature of particle-surface interactions during CMP, are often inadequate for simulating or explaining CMP removal rates [Ste99, Kne97]. Instead, transient techniques such as chronoamperometry that resolves millisecond range can provide better correlation with CMP removal rates [Sin02]. Lee extensively characterized chemical interactions during copper CMP [Lee03].

The rapid formation of a thin passive layer is one of the key aspects for achieving planarization [Sin02]. For this reason, an oxidizer is normally added to form a passive layer for metal CMP. However, hydrogen peroxide (H_2O_2), an oxidizer itself, is known to be inefficient in passivating copper surfaces. A corrosion inhibitor such as benzotriazole can be added to form a thin passive layer. By properly adjusting concentration of peroxide and benzotriazole, we can control the thickness of the surface passvation layer. Benzotriazole (BTA, $C_6H_5N_3$), Citric acid (CA, $HO_2CCH_2C(OH)(CO_2H)CH_2CO_2H$).

Indentation Depth of Single Particle (δ_W)

A model describing the indentation degree of particles onto the surface during polishing was first developed by Cook and Brown et al. [Bro81] for the super polishing of metals. The particle indentation can be described by a model in which a spherical particle of diameter ϕ under uniform load P penetrates the surface with a force L and moves along the surface at some velocity removing a volume of material of dimensions proportional to the penetration. They utilized a standard Hertzian indentation to describe the penetration degree of the particle into the substrate. The indentation depth of a single particle was expressed as

$$\delta_w = \frac{3}{4} \cdot \phi \cdot \left(\frac{P}{2 \cdot K \cdot E} \right)^{2/3} \qquad (2.13)$$

This equation assumes that the particles are much harder than the surface layer and interfacial contact between the particles and the surface is elastic.

Zhao et al. and Qin et al. [Zha02, Qin04] defined the indentation depth of a particle into the wafer by making use of the theory of contact mechanics in conjunction with the force equilibrium of a particle participating in the wear process. Different modes of deformation caused by a single particle into the pad (elastic) and wafer (plastic) due to their very different mechanical properties. Based on these modes, the wafer/particle/pad contact within the real area of contact between the pad and the wafer can be visualized in Fig. 2-9, where the particle is largely embedded into the pad surface. The elastic contact force between the pad and the particle (F_{SP}) is given by

$$F_{SP} = \frac{4}{3} E_{SP} \left(\frac{\phi}{2} \right)^{1/2} {\delta_P}^{3/2} \qquad (2.14)$$

where E_{SP} is the reduced Young's modulus of contacting bodies, pad and particle, and δ_P is indentation depth of a particle in polishing pad. The plastic contact force (F_{SW}) between the wafer and the particle by

$$F_{SW} = H_W \pi \phi \delta_W \qquad (2.15)$$

where H_W is wafer hardness, and δ_W is indentation depth of a particle in wafer. This force equilibrium can be used to calculate the indentation depth (δ_W) of the particle into the wafer surface with knowledge of wafer hardness, particle diameter and Young's moduli of the particle and pad.

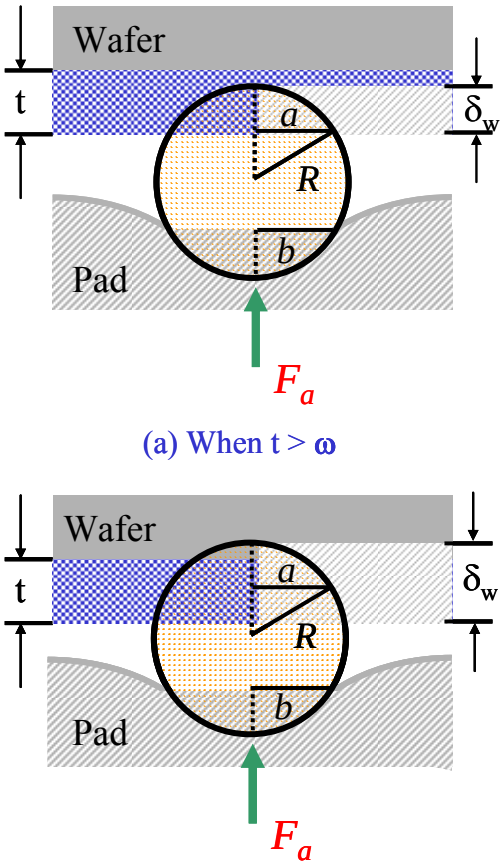

Figure 2-9 The wafer-particle-pad interaction during polishing. This schematic shows a single particle that is trapped between the pad and the wafer surface (a) when the indentation depth, δw, of the particle is smaller than the surface layer thickness, t, and (b) when the indentation depth is greater than the surface layer thickness [Qin04].

CHAPTER 3
EXPERIMENTALS

This chapter illustrates various experimental methods used in this investigation. Preparation processes for polishing experiments such as slurry characterization, polisher calibration, and various analysis methods for polishing experiments such as removal rate measurements, surface roughness measurements, and in situ friction force measurements are described in detail. Brief descriptions of measurement principles for each equipment are presented.

Sample Preparation

Wafer Preparation

8-inch blanket PVD copper/Ta/TEOS silica wafers were cleaved into 1.5 in. x 1.5 in. square specimens. To prevent edge chipping during the polishing, the specimen edges were rounded with silicon carbide grinding papers (Buehler, Grit 400/P800). The specimens were then cleaned with methanol and acetone and then dried with blown air.

Particle Characterization and Slurry Synthesis

The size, size distribution, and shape of the abrasive particles were characterized using various techniques. The light scattering method was used to measure the size and distribution of the particles, and imaging techniques such as scanning electron microscopy (SEM) and transmission electron microscopy (TEM) were used to verify the size and shape of the particles.

Light Scattering

A Microtrac UPA 150, the light scattering particle size analyzer, supplied by Honeywell was used to measure the particle size distribution. The light scattering is a relatively simple method that provides accurate information (0.003 μm to 6.54 μm) on the particle size and the size distribution. Light from laser diode is coupled to the sample, scattered from each particle, and shifted by particle motion. The velocity distribution of particles suspended in a dispersing medium is a known function of particle size. The shifted scattered light is mixed with coherent unshifted light in a silicon photodetector and mathematically analyzed with interfaced software.

The particles were diluted in deionized water and sonicated for 10 minutes before the measurements. The measurements were repeated multiple times to obtain reproducible results.

Imaging Techniques

Particle size and shape were confirmed by microscopic techniques such as transmission electron microscopy (TEM) and scanning electron microscopy (SEM). The TEM was utilized for small-size particles (30 nm diameter) that are not easily observable with the SEM technique. Corresponding histogram of particle distribution to the TEM images was also plotted by numbering and sizing particles in Photoshop.

Slurry Preparation

Any visible reactions while mixing different chemicals and particles were carefully monitored. Proper handling, such as sufficient stirring rate and time when mixing the polishing additives, was done. First, citric acid and benzotriazole (BTA) were mixed in deionized (DI) water. Abrasive particles were diluted for a desired solids loading (weight %) in separate DI water and were sonicated for approximately 10 min. to break down the

aggregated particles to primary particles. The chemicals (citric acid and BTA) and abrasive particles were mixed into one container, and its pH was adjusted by KOH. Hydrogen peroxide was always added prior to each polishing in order to minimize the effect of time dependent degradation.

Table-Top Polishing Equipment

Polishing experiments were performed on tabletop polishing equipment (Struers RotoPol-15 and RotoForce-1) using IC 1000/Suba IV stacked pads (Rodel). Such systems realistically represent scaled-down versions of industrial scale system.

Substrate Holder

Figure 3-1 shows schematics of the table-top polishing equipment and the substrate holder. The sample holder was specially machined for the RotoForce-1. As shown in Fig. 3-1b, the holder was designed to have three rods (the fixation rods to the polisher head, RotoForce-1) for obtaining even pressure distribution. An adhesive carrier film (Rodel) was attached in the square-shape recessed area to hold the wafer against the pad.

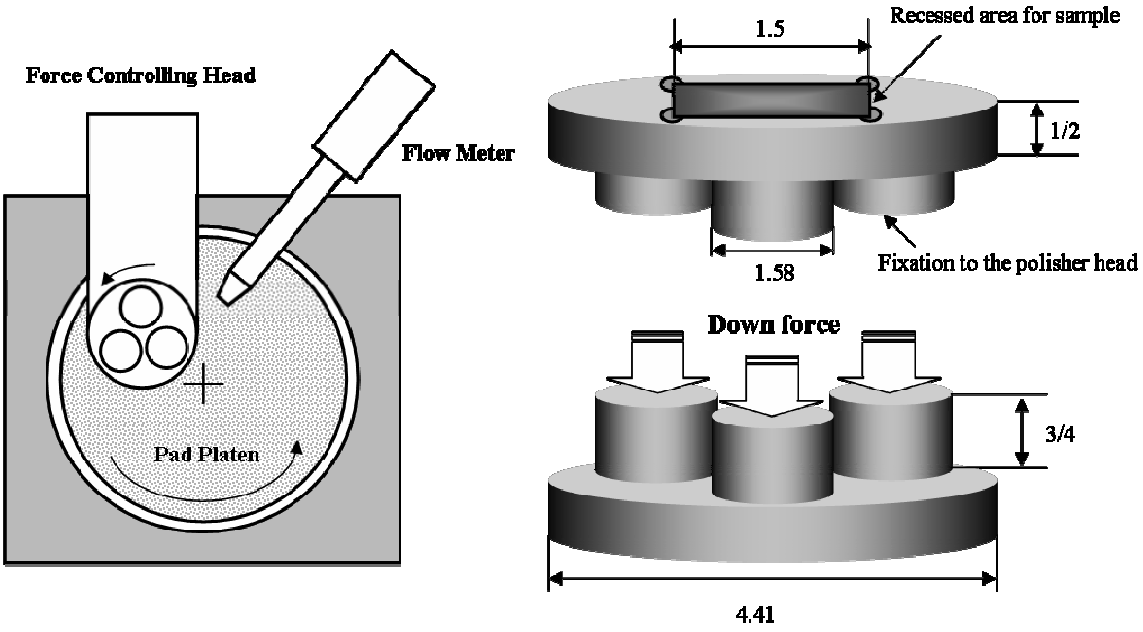

(a) (b)

Figure 3-1 Schematics of (a) table-top polishing equipment and (b) the substrate holder, bottom view (upper image) and top view (lower image)*.

Polishing Equipment Calibration

An operational pressure range of a bench-top polishing apparatus was calibrated using a weight balance to provide accurate control of down pressure (Fig.3-2a), and the apparatus was benchmarked using commercially available CMP slurries and comparing our experimental results with results from open literature [Zho02] (Fig.3-2b). TEOS Silica wafers were used as standard samples. The bench-top polisher turned out to be reliable.

* Inch scale. The figure does not represent the real scale.

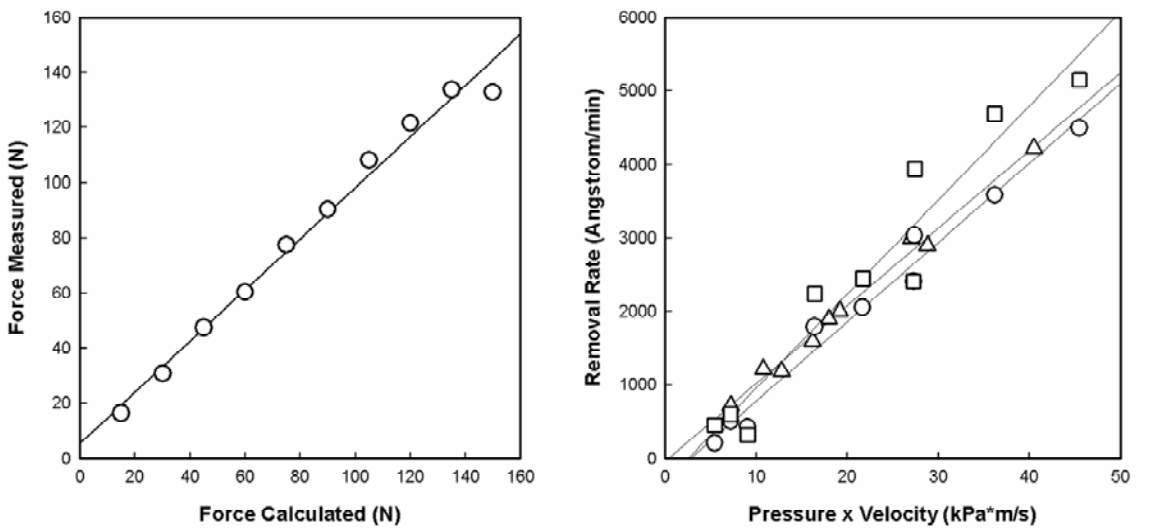

(a) (b)

Figure 3-2 The polishing equipment calibration (a) down force calibration using weight balance (b) benchmarking of the table-top polisher by comparing removal rate values as a function of pressure*velocity (open circles represent in this study (open circle) with data from open literature (open triangle [Zho03]) and commercial slurry (open square, Klebosol, Rodel).

Polishing Experiments

The pad was conditioned prior to each polishing experiment using a grid-abrade diamond pad (Rodel). The down pressure was varied from 1.5 psi to 9.0 psi. The speed of both platen and head were fixed at 150 RPM (0.88 m/s). The flow rate was fixed at 100 mL/min. Polishing was carried out for 30 seconds, and repeated three times. One-hour static etch rate was measured with the four-point probe method before and after dipping specimens in the aqueous media.

Table 3-1 Comparison of process variables and slurry ingredients for calibration.

	Zhou et al. [Zho02]	In this study	Klebosol (Rodel ILD)
Abrasive type	Colloidal silica	Colloidal silica	Colloidal silica
Abrasive size	80 nm	80 nm	~ 100 nm
Solids loading	30 wt.%	30 wt.%	30 wt.%
pH	11.0	10.5	10.8
Media	DI water	DI water	-----
Polishing apparatus	RotoPol-35	RotoPol-15	RotoPol-15
Prestonian constant (K_p)	107.94	105.65	127.83

Table 3-2 Process parameters for calibration.

Down Pressure	1.5 to 9.0 psi
Head Speed	150 RPM
Platen Speed	150 RPM
Slurry Flow Rate	100 mL/min
Polish Time	30 sec

In Situ Friction Force Measurements

The in-situ friction force measurement is a powerful technique for examining polishing mechanisms. Fig. 3-3 shows the schematic of the force measurement apparatus. The force transducer was connected to a data acquisition system and data was recorded every 250 ms for duration of 60 seconds. This apparatus has been extensively used by our CMP group to investigate polishing-scale friction force behavior [Mah99a, Mah99b, and Cho04] especially in silica polishing. To explore various interactions in copper polishing, experiments were conducted as a function of particle size, concentration, and chemical additives with fixed values of the rest of the polishing parameters, such as pressure, velocity etc. The friction force values were correlated with the copper removal rate values.

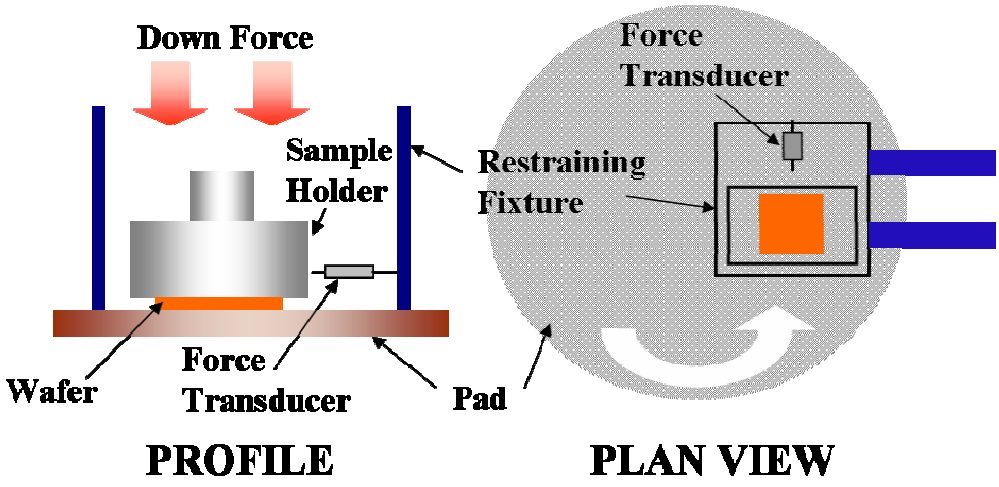

Figure 3-3 Schematic of apparatus for in situ friction force measurement [Mah99].

Film Thickness Measurements

Removal rates were determined by measuring the film thickness before and after polishing. The copper film thickness was measured using sheet resistance measurements and the thickness of insulating silica dielectrics used for calibrating the table-top polisher was measured using Various Angle Spectroscopic Ellipsometry (VASE).

Four Point Probe Method

The four point probe technique (Jandel) was used to measure sheet resistance and ultimately to determine the thickness of copper films. As shown in Fig. 3-4, a four point probe setup is mainly composed of current source, digital voltmeter, and four point probes. The four point probes consist of two current carrying probes (1 and 4) and two voltage measuring probes (2 and 3). The metal probes are lightly pressed onto the copper surface. A constant current (I) is passed through probes 1 and 4 and then the resulting voltage drop (V) between probes 2 and 3 is measured. The sheet resistance of film (R_s) is expressed as

$$R_s = K \cdot \frac{V}{I} \tag{3.1}$$

where K is a correction factor dependent on the specimen diameter and probe spacing. If the probe spacing is larger than the film thickness (t) and smaller than the distance to edge of the film, K=4.53.

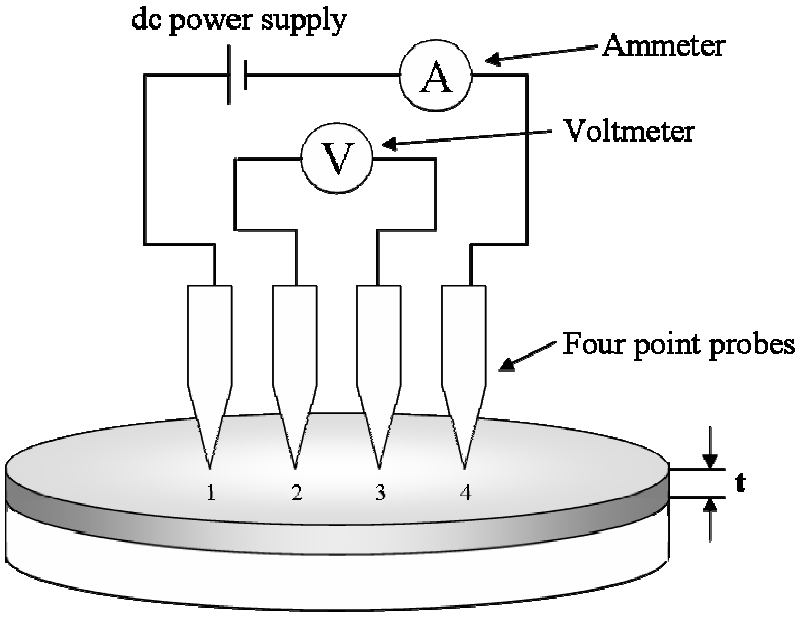

Figure 3-4 Schematic of four point probe measurement.

The sheet resistance is film-dependent quantity which is rearranged from resistance. Let us consider resistance of a bar of materials with resistivity ρ. In this rectangular bar with thickness t, width W, and length L, the resistance is given by

$$R = \rho \cdot \frac{L}{A} = \rho \cdot \frac{L}{W \cdot t} = \rho/t \cdot \frac{L}{W} = R_s \cdot \frac{L}{W}$$

where $R_s = \rho/t$ is the sheet resistance of a layer of this material. Thus one can obtain the thickness of the copper film by measuring the sheet resistance of the copper film.

Various Angle Spectroscopic Ellipsometry (VASE)

Ellipsometry is a non-destructive technique for determining optical constants, film thicknesses in multilayered systems, surface and interfacial roughness, etc [Bru92]. In this study, the ellipsometry was used to measure the thickness of silica films that were used for calibrating the table-top polisher. Fig. 3.5 shows the schematic of spectroscopic ellipsometry (J.A. Woollam Co. Inc.).

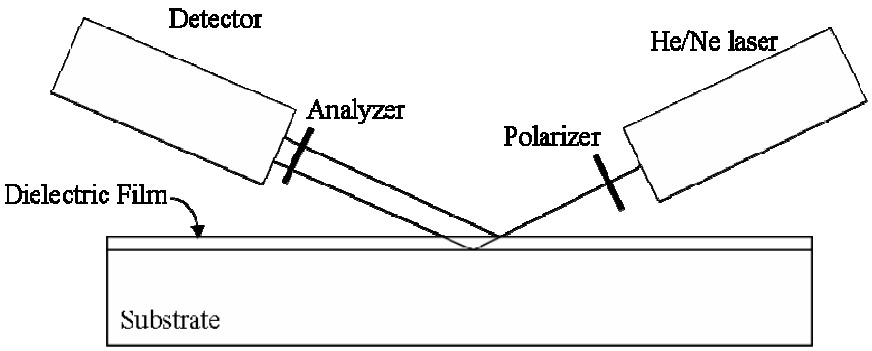

Figure 3-5 Schematic illustration of spectroscopic ellipsometry [Bru92].

Ellipsometry measures relative changes in the amplitude,ψ, and the phase difference, Δ, of a linearly polarized monochromatic incident light upon an oblique reflection from a sample surface. In the ellipsometry, the complex ratio, ρ, is defined by the following equation,

$$\rho = \frac{R_p}{R_s} = \tan\psi \cdot \exp i\Delta$$

where R_p *and* R_s are the complex reflection coefficients of the polarized light parallel and perpendicular to the incident plane, respectively. For a layered sample, measured spectra may be analyzed using an appropriate fitting model constructed based on the sample

structure. In the model, unknown parameters, such as thickness, refractive index and absorption index of a layer may be then determined as fitting parameters. These parameters are then determined by minimizing the mean-squared errors (MSE) between measured and calculated data. In order to obtain thickness information, the technique requires a 'model' that contains wavelength of incident light, incident beam polarization state, angle of incidence, thickness of layer, optical constants (refractive index, absorption index, etc.). The thickness input values are varied until we meet perfect match with the model.

Surface Topography Measurements: Atomic Force Microscopy (AFM)

Atomic force microscopy (Digital Instrument Nanoscope III) was used to measure the surface roughness of polished copper specimens. The schematic diagram of the AFM apparatus is shown in Fig. 3-4. The AFM utilizes a sharp probe (a tip mounted on a flexible cantilever) moving along the specimen surface in a raster scan. Repulsive van der Waals forces between atoms on the tip and substrate cause deflection of the cantilever. The force between the tip and sample are a function of the separation distance. Therefore, surface topography is obtained by monitoring the cantilever deflection. The light from the laser diode is reflected upon the cantilever and detected on the quadruple photodiode. By measuring the light position on the photodiode, changes in the bending of the cantilever can be measured. The surface roughness is quantitatively expressed as

$$RMS = \sqrt{\frac{1}{n} \cdot \sum_{i=1}^{n} (Z_i - Z)^2} \tag{3.1}$$

where Z_i is the height values of single data points in the image, Z is the mean value of all height values in the image, and n, the number of data points within the image.

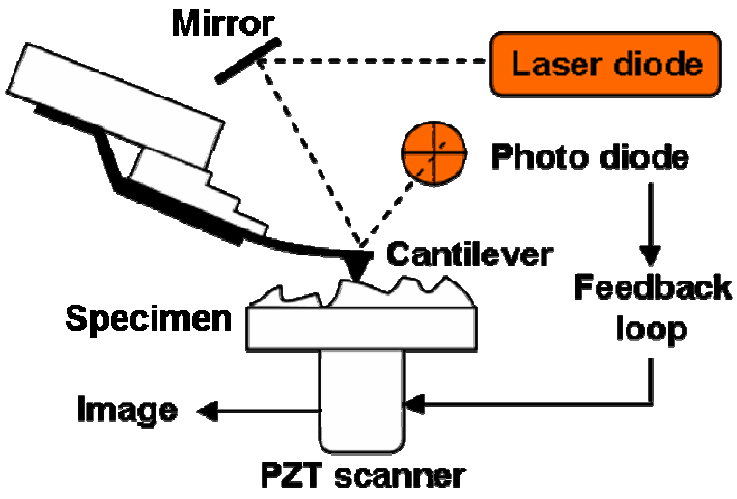

Figure 3-6 Schematic diagram of atomic force microscopy (AFM) [Bru92].

The measurements were conducted in tapping mode. Prior to all surface roughness measurements, excess particles adhered on the surfaces after polishing were removed by sonicating for a minute in isopropanol.

CHAPTER 4
SYNERGISTIC CHEMICAL-MECHANICAL EFFECTS

As addressed in chapter 1 and 2, due to their fragility and poor adhesion next generation interconnect materials such as copper and low k dielectrics are susceptible to CMP-induced contact stresses (normal and shear) which may lead to defect formation such as microscratches, copper and barrier layer delamination, low k damage, dishing and erosion [Sin03, Wan01].

To reduce the defect formation, investigations such as reduction in down pressure [Kon03], abrasive-free polishing [Pad03], electro-polishing [Cha03], etc. have been conducted. Material removal by these methods, however, is often dependent on chemical dissolution for high removal rate, which is known to be ineffective for obtaining high planarity due to its isotropic nature.

Our methodology in this study to address the defect reduction is based on contact mechanics. In this mode of polishing regime, it is believed that active abrasive particles are trapped between pad asperity and wafer surface, and therefore participate in material removal. As shown in Fig. 2, the particle indentation during polishing is a nano-scale phenomenon and its depth into the wafer surface can be theoretically estimated using force equilibrium between particle-pad interface and particle-wafer interface [Zha02, Qin04]. This penetration depth depends on (i) particle properties (size, hardness, shape etc.), (ii) surface layer properties (thickness, hardness, density, etc.), and (iii) pad modulus. It should be noted that the penetration depth could be either larger or smaller than the surface layer thickness. Due to the low hardness of bare copper underneath the

surface layer, a penetration depth greater than the surface layer thickness can cause significant micro-scratches and other defect. Therefore, the defect formation can be minimized by decreasing the penetration depth of particles. According to the concept above, however, the penetration depth is not determined solely by the particle properties, but is determined by their synergistic interaction with surface layer that can be influenced by various factors. A study of the particle effects on polishing characteristics with systematic variation in slurry chemistry is critical, but has yet to be investigated.

Our objective in this chapter is to examine the synergistic chemical-mechanical effects on defect formation during copper CMP. To explore the effects of particle size and hardness, various types of particles such as 100 nm silica particle, 1 micron silica particle, and 200 nm alumina particle were used. Slurry chemistries such as hydrogen peroxide as an oxidizer, benzotriazole as a corrosion inhibitor, and citric acid as a chelating agent were also systematically varied to alter the copper surface properties (pH: 7.0). Removal rate and surface roughness were measured as function of these slurry parameters. The surface roughness and micro-scratches were used as indicators of defect formation. Based on measurement results, the proper method to obtain “gentle” polishing behavior of copper is suggested.

Particle Characterization

To study the effect of particle size and hardness, three different types of particles (nano-size silica, micron-size silica, 200 nm alumina) are used in this chapter. The details of the particles used in this chapter are given in Table 4-1.

Table 4-1 Details of different types of particles

Materials	Approx. mean diameter (μm)	Manufacturer	Type
SiO2	0.1	H.C. Starck	Levasil
SiO2	1.0	Geltech	Geltech 1.0 μm
α-Al2O3	0.2	Sumitomo	AKP 50

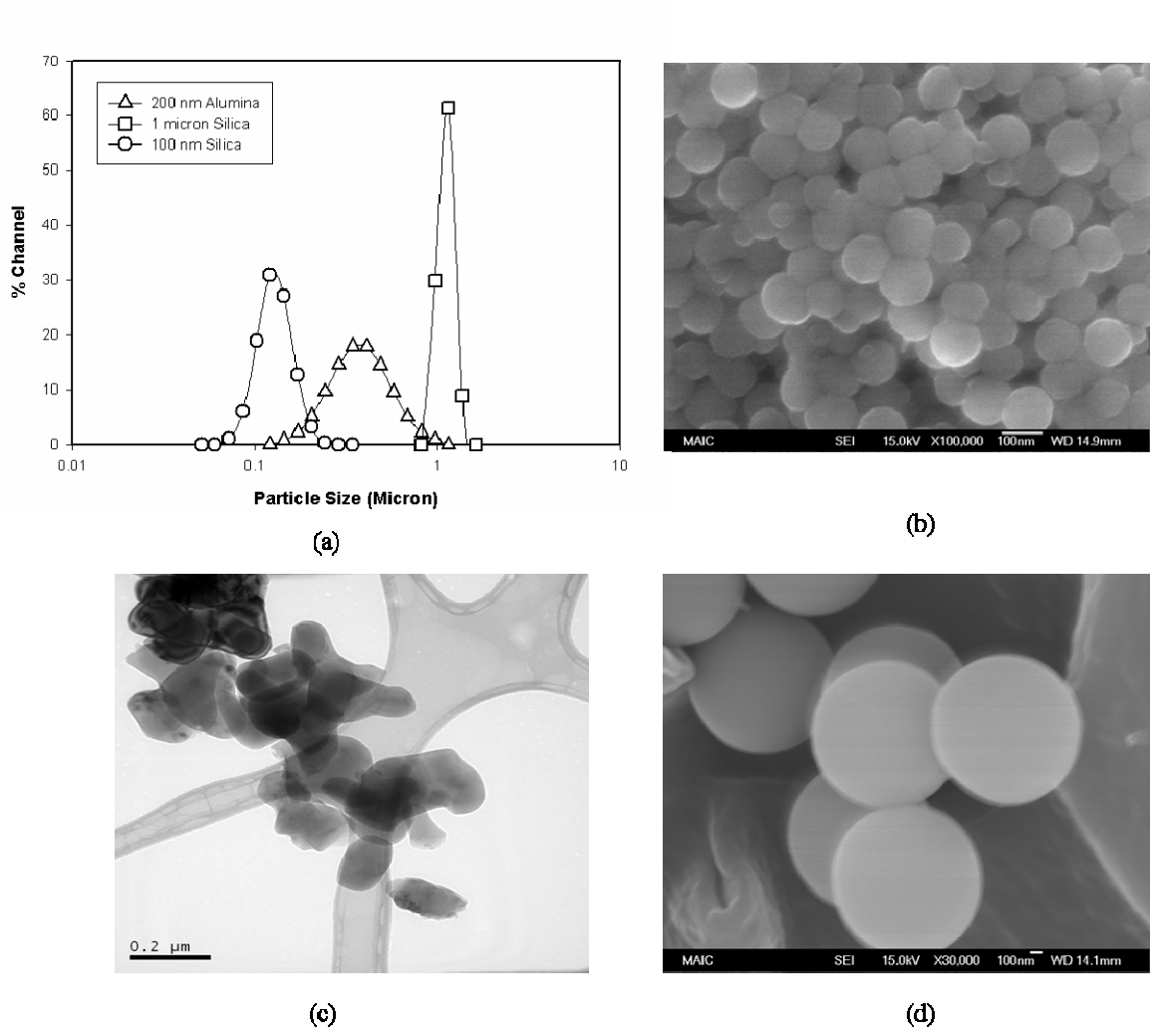

Figure 4-1 Particle analysis (a) particle size distribution obtained by light scattering method (b) image of 100 nm silica particle obtained by SEM (c) image of 200 nm alumina particle obtained by TEM (d) image of 1 μm silica particle obtained by SEM.

Prior to polishing experiments, the particles used were characterized using several techniques. The light scattering method was used to determine the particle size and the particle size distribution. The imaging techniques such as SEM and TEM were used to confirm the particle size and shape. The analysis results are shown in Fig. 4-1. Fig. 4-1a shows the particle size distribution of three different particles obtained by light scattering method. Figures 4-1b to 4-1d show the images of the particles obtained by SEM and TEM. The silica particles (100 nm and 1 μm in mean diameter) are quite spherical whereas the alumina particles are somewhat irregular and faceted in shape.

Colloidal Silica Nanoparticles

Figure 4-2 shows the removal rate of copper using neutral slurries (pH 7.0) with 10 wt. % solids loading of colloidal silica particles. As shown in Fig. 4-2a, the removal rate obtained by the nanoparticles dispersed in de-ionized water is approximately 15 nm/min, which is quite negligible. The addition of hydrogen peroxide does not significantly influence the removal rate. Figure 4-2b shows the effect of benzotriazole addition in 5 % hydrogen peroxide on removal rate, which suggests that the removal rate is still quite low.

Figure 4-3 shows the removal rate measured as a function of citric acid concentration in the same slurry used for Fig. 4-2b. In the presence of 5 % hydrogen peroxide and 10 mM benzotriazole, the increase in citric acid concentration in the slurry exhibits a linear increase in removal rate. The figure also shows that the removal rate is quite low when only citric acid is added in de-ionized water without addition of hydrogen peroxide and benzotriazole.

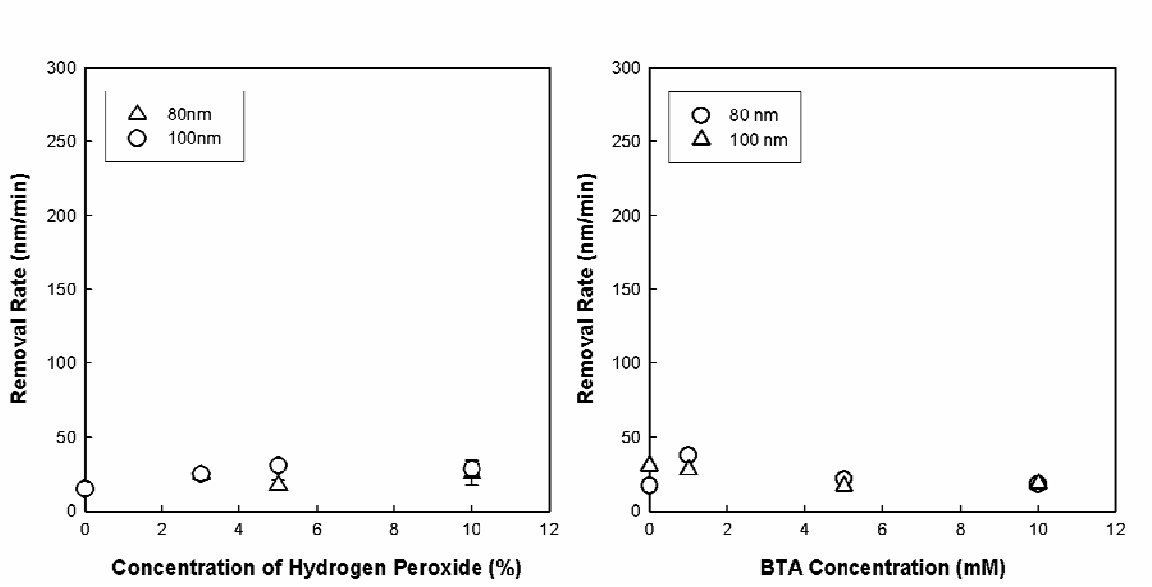

(a) (b)

Figure 4-2 Removal rate of copper using 10 wt. % solids loading of colloidal silica particles at pH 7.0 (a) effect of hydrogen peroxide concentration in de-ionized water (b) effect of benzotriazole concentration in 5 % hydrogen peroxide.

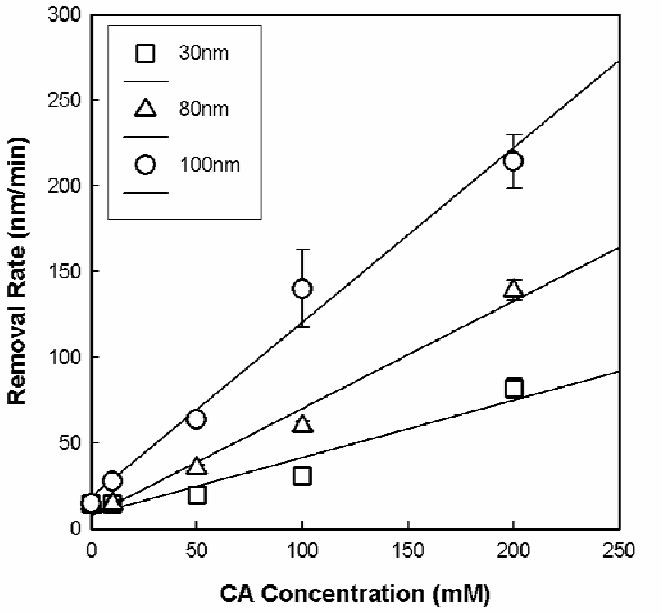

Figure 4-3 Removal rate of copper versus citric acid concentration, pH: 7.0. 100 nm silica particles are used. Open circle indicates the removal rates measured with 5 % H_2O_2 and 10 mM benzotriazole. Open triangle indicates the removal rate measured in water.

Figure 4-4 shows the root mean square (RMS) values of copper surface after polishing with 10 mM and 200 mM of citric acid concentration in the slurry used for Fig. 4-3. The result shows that the surface roughness is fairly independent of citric acid concentration

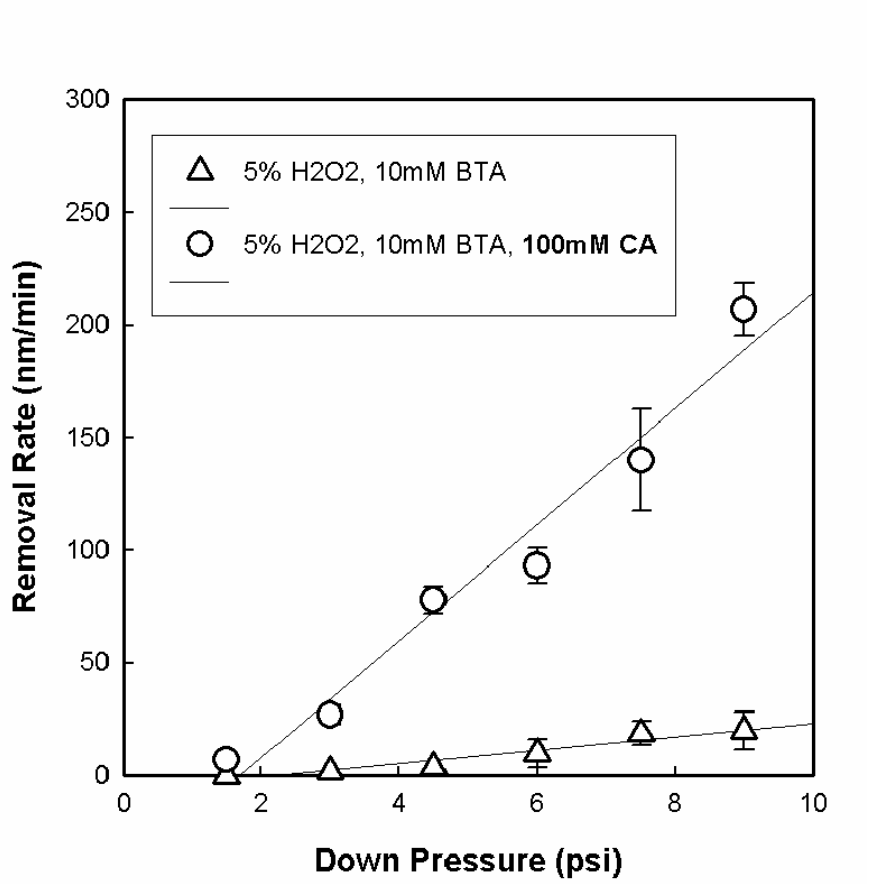

Figure 4-4 Removal rate of copper as a function of down pressure with and without 100 mM citric acid. 5 % hydrogen peroxide, 10 mM benzotriazole 100 nm silica at 10 wt. %, pH: 7.0.

Figure 4-4 shows the removal rate of copper as a function of down pressure using 100 nm silica particles at 10 wt. % along with 5 % H_2O_2, 10 mM benzotriazole (BTA) and 100 mM citric acid at pH 7. Without citric acid, the removal rate is low, below 30 nm/min, over the entire down pressure range. However, as 100 mM of citric acid is added to the slurry, the removal rate increases considerably. The linear increase in removal rate

with increasing down pressure is attributed to an increase in the number of active particles contacting the wafer surface due to the compliant nature of the polymeric pad.

Based on these results, it is suggested that the addition of citric acid may enhance delamination between the surface layer and the bulk copper, and may cause brittle fracture by the abrasives making it possible to form a layer 'removable' by the nano-size silica abrasives. As shown in Fig. 4-5, the surface topography after polishing with nano-size silica abrasives is almost scratch-free, indicating that material removal takes place only within the surface layer. Slight increase in root mean square (RMS) value is shown as down pressure increases. The linear increase in removal rate and slight increase in RMS as a function of the down pressure are attributable to an increase in the active number of abrasives in contact with the wafer surface, due to the compliant nature of the polymer pad [4].

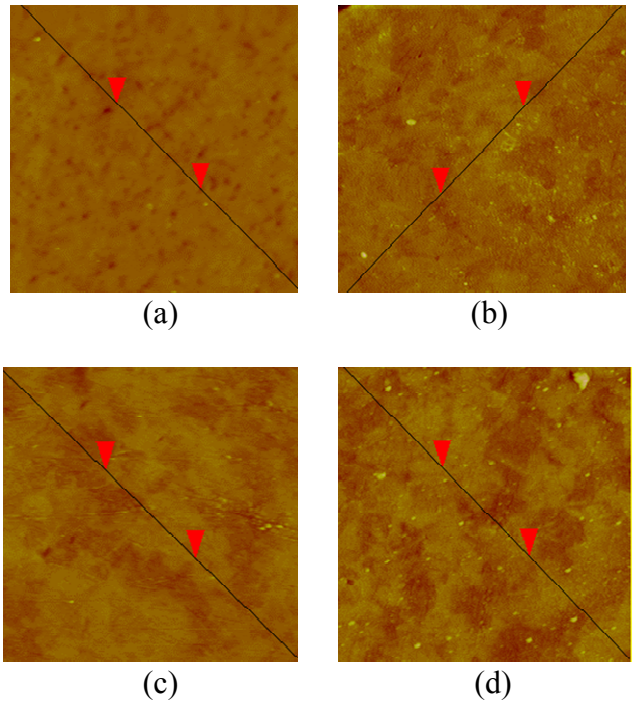

Figure 4-5 Down pressure effect on surface image and roughness after polishing with 100 nm silica particles at 10 wt. %: (a) 1.5 psi (RMS: 0.350 nm), (b) 4.5 psi (RMS: 0.427 nm), (c) 7.5 psi (RMS: 0.711 nm), (d) 9.0 psi (RMS: 1.189 nm).

The rapid formation of a thin passive layer is one of the key aspects for achieving excellent planarity by the CMP process [Sin02]. For this reason, an oxidizer is normally added in copper polishing slurries. The oxidizer such as hydrogen peroxide is responsible for rapidly forming the passive layer. However, hydrogen peroxide itself is known to be inefficient to passivate the copper surfaces. A corrosion inhibitor such as benzotriazole can be added to form a thin passive layer. As shown in chapter 2, the thickness of the surface passive layer can be controlled by properly adjusting concentration of peroxide and benzotriazole. However, using nano-size silica particles, the removal rate for this slurry condition is very low. This implies that the surface layer formed by hydrogen peroxide and benzotriazole is mechanically too rigid to be removed by nano-size silica particles. On the other hand, the synergistic effect is found with the addition of citric acid in the slurry and serves to increase the removal rate considerably.

Micron-size Silica and 200 nm Alumina Particles

Unlike in nano-silica based polishing, microscratches are often observed after polishing of copper with hard or large abrasive-based conventional slurries most likely due to the penetration deeper than the surface layer thickness. This removal behavior resembles conventional mechanical polishing where the removal of material results from direct interaction between abrasives and the bare copper, i.e. the indentation of the surface and the removal of material by a scratching process is prevalent [Sin02b]. As shown in Fig. 4-6, polishing with 200 nm alumina abrasive generates a much higher removal rate than that of 100 nm silica abrasive, but shows very aggressive microscratches (Fig. 5) with high RMS value.

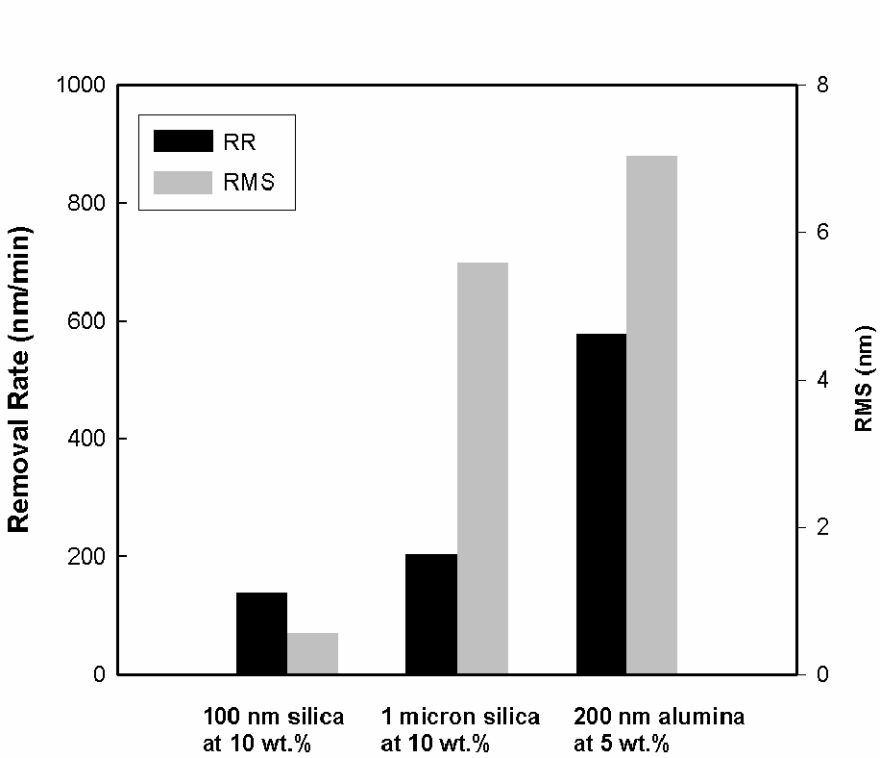

Figure 4-6 Removal rate and surface roughness after polishing with various particles (slurry condition: 5 % H_2O_2, 10 mM BTA, 100 mM citric acid at pH 7.0)

The results indicate that the hard abrasives not only penetrate through the surface layer, but also remove bare copper effectively with the scratching process that requires higher energy to break copper bonds. On the other hand, polishing with 1 μm silica abrasives does not exhibit much higher removal rate than that of 100 nm silica abrasives. The RMS value of the copper surface after polishing with the micron-size silica is slightly lower than that obtained from 200 nm alumina abrasives, but much higher than that obtained from 100 nm silica abrasives. This suggests that the large silica abrasive can penetrate through the surface layer but cannot effectively remove bare copper underneath the layer due to its low hardness. As such, the removal mechanism can be quite different when indentation depth by the abrasive is larger or smaller than the surface layer thickness. In order to achieve low stress polishing of copper, it is preferable to cause

brittle fracture only within the surface layer because it requires low energy to generate material removal due to nature of brittle fracture.

Conclusion

We have investigated copper CMP using nanoparticle-based slurries. With addition of citric acid in the presence of hydrogen peroxide and benzotriazole at pH 7, we obtained moderate removal rates with very low rms values, less than 0.7 nm. Micron-size silica and 200 nm alumina particles were also used as comparison.

1. The hardness and size of the particles can be reduced to lower the penetration depth, thus avoiding damaging effects. However, reducing particle hardness and size without use of synergistic chemistries may lead to much reduced removal rates.
2. The addition of complexing agent, citric acid, in the slurry is critical to the formation of surface layer removable by the colloidal silica nanoparticles.
3. In contrast, larger or harder particles result in greater surface defects suggesting that removal takes place via scratching process.

We propose that citric acid softens the surface layer formed by hydrogen peroxide and benzotriazole, and results in larger indentation depth of nano-size silica particles, thus increasing the removal rate. Combined mechanical-chemical effects are needed to achieve low-defectivity polishing of copper.

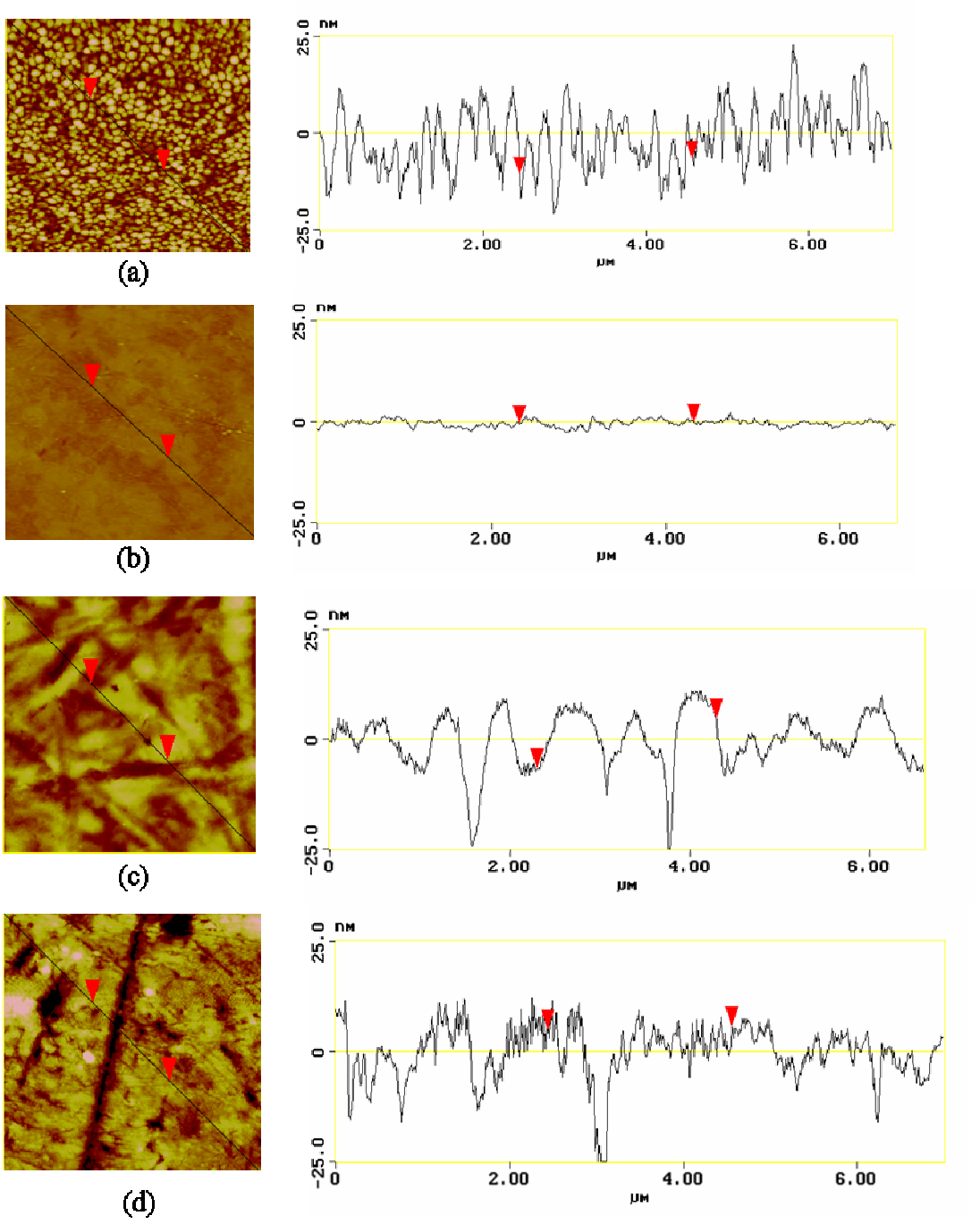

Figure 4-7 Surface roughness copper specimen (a) as received (RMS: 6.963 nm) copper wafer (b) polished with 100 nm silica at 10 wt. % (RMS: 0.711 nm) (c) polished with 1 μm silica at 10 wt. % (RMS: 6.985 nm) (d) polished with 200 nm alumina at 5 wt. % (RMS: 8.793 nm)

CHAPTER 5
FORMATION OF REMOVABLE SURFACE LAYER

In chemical mechanical polishing (CMP) of copper, chelating agents are often added in the hydrogen peroxide, the most commonly used oxidizer, -based slurries to increase the removal rate [Sin02b]. It has been reported that simultaneous use of some chelating agents and the peroxide synergistically increases the removal rate of copper. These results are normally inferred to the ability of the chelating agents to form copper complexes and its enhanced solubility [Aks02, Aks03, Du04, Che04].

Citric acid is of particular interest in this work because, although it is often utilized in copper CMP due to its chelating ability, it is relatively less explored among other chelating agents such as glycine. Tamilmani et al. [Tam02] constructed potential-pH diagrams based on thermodynamic calculations and suggested that presence of the citrate ions in the slurry would tend to chemically dissolve copper through complex formations. Chen et al. [Che04] studied the effect of citric acid on copper polishing using hydrogen peroxide-based acidic slurries that contain 50 nm alumina particles. The removal rate in their study was exceedingly high, which was up to 5.5 μm at 3 psi. It is conceivable that the enhanced material removal in acidic regime without an inhibitor may include an unwanted level of chemical dissolution, which would not help in achieving efficient planarization due to its isotropic nature and also raises a corrosion issue. In addition, we demonstrated in chapter four that use of such hard particles may result in significant micro-scratches due to their severe penetration and direct interaction with soft bare

copper underneath the surface layer. Therefore, further aspects of citric acid addition under more passivating and mechanically gentle ambient should be addressed.

Our objective in this chapter is to understand the role of citric acid during the copper CMP using silica nanoparticle based neutral slurries. To study its effect on polishing behavior, removal rate was measured as a function of citric acid in the presence of hydrogen peroxide and benzotriazole at pH 7. Static etch rate measurements and potentiodynamic scans were conducted to study dissolution / passivation behavior. To study the effect of citric acid on chemical composition of the surface layer, x-ray photoelectron spectroscopy (XPS) was used. Reaction kinetics of the layer formation was studied using chronoamperometry technique. Physical properties of the surface layer such as hardness and density were obtained using nanoindentation and x-ray reflectivity (XRR), respectively. Various aspects of citric acid addition on copper surface and its influence on polishing performance are discussed.

Experimentals

Removal Rate and Static Etch Rate Measurements

Eight-inch blanket PVD copper/Ta/TEOS silica wafers were cleaved into 1.5 in. x 1.5 in. samples. Polishing experiments were conducted on tabletop polishing equipment (Struers RotoPol-15 and RotoForce-1) using IC 1000/Suba IV stacked pads (Rodel). The pad was conditioned prior to each polishing experiment using a grid-abrade diamond pad (Rodel). Down pressure was fixed at 7.5 psi, with 150 RPM of both platen and head speed (0.88 m/s). Flow rate was fixed at 100 mL/min. The sample holder was designed and machined for the equipment. An adhesive carrier film (Rodel) was attached in the square-shape recessed area to hold the wafers against the pad. Removal rates were determined by measuring the thickness of the copper layer using the four-point probe

method before and after polishing. Polishing was carried out for 30 seconds, and repeated three times. Chemicals (hydrogen peroxide, citric acid and benzotriazole) and abrasive particles were mixed in deionized water, and further adjusted to pH 7.0 by KOH. One-hour static etch rate was measured with the four-point probe method before and after dipping specimens in the aqueous media.

Electrochemical Tests

The three electrode cell was used. High purity copper coupons (99.9985%), the working electrode, were pre-polished and mounted in a Teflon holder that exposed 1 cm^2 surface area. A saturated calomel electrode (SCE) and two graphite rods was used as a reference electrode and counter electrodes, respectively. The Autolab PGSTAT 30 was used for the potentiodynamic scans. The scans were performed at the same rate of 1 mV/s, beginning at -0.75 V and ending at 0.5 V (respect to SCE). To examine the transient electrochemical behavior, the FRA2 module was added to the potentiostat. This technique, so-called Chronoamperometry, measures the decrease in current with time at a given electrical potential, which provides valuable time-resolved information. Prior to the measurement, the copper specimens were kept at a cathodic potential in the test solution to prevent oxidation reaction on the surface. Then an open-circuit potential, measured from potentiodynamic scans, was applied. The current drop was monitored in the millisecond range and converted to the surface layer thickness using Faraday's law of electrolysis.

X-ray Photoelectron Spectroscopy (XPS)

XPS experiments were performed to determine the chemical composition of the chemically modified surface layer. A specimen was dipped in the aqueous solution for a minute and moved over to the ultra high vacuum (UHV) chamber that was less than 10^{-8}

Torr. Photoelectrons were excited by using non-monochromatized Mg Kα x-ray irradiation (1253.6 eV), and the detection angle was normal to the sample surface.

Nanoindentation and X-ray Reflectivity

Nanoindentation experiments were conducted using a cube corner diamond indenter with Triboindenter and Triboscope manufactured by Hysitron. Copper specimens were dipped in the aqueous solutions for a minute and moved to the sample stage. For each specimen, the experiments were conducted at 64 separate maximum loads starting from 100 μN to 5 μN with successive 4 % decrease. All indentations were performed using a load-time sequence. To characterize the density of the surface layer modified by the chemical additives, x-ray reflectivity (XRR) was used. XRR is a non-destructive and non-contact technique for density measurements. A Philips X'Pert x-ray diffraction system was used for this study. For x-ray radiation of incident angle $\theta_I <$ critical angle (θ_c) total external reflection occurs at a certain reflection angle (θ_r). The critical angle is proportional to the half power of the layer density. For conditions in which the incident and reflected angle are equal, the density can be obtained for the chemically modified surface layer.

Synergistic Chemical Effect

Figure 5-1 shows the removal rate of copper vs. citric acid concentration (0-200 mM) using 10 wt. % of 100 nm silica particles along with 5 % H_2O_2 and 10 mM benzotriazole (BTA) at pH 7. The peroxide and BTA are added in the slurry for the purpose of rapid formation of a passive layer which is necessary for achieving the effective planarization [1]. As shown in Fig. 5-1, the removal rate of these two chemical agents without citric acid is negligible but linearly increases with an increase of citric acid concentration in the

slurry. The figure shows that the removal rate is also influenced by the down pressure. To identify the role of citric acid, as the third chemical ingredient that increases the removal rate, several experiments were further conducted.

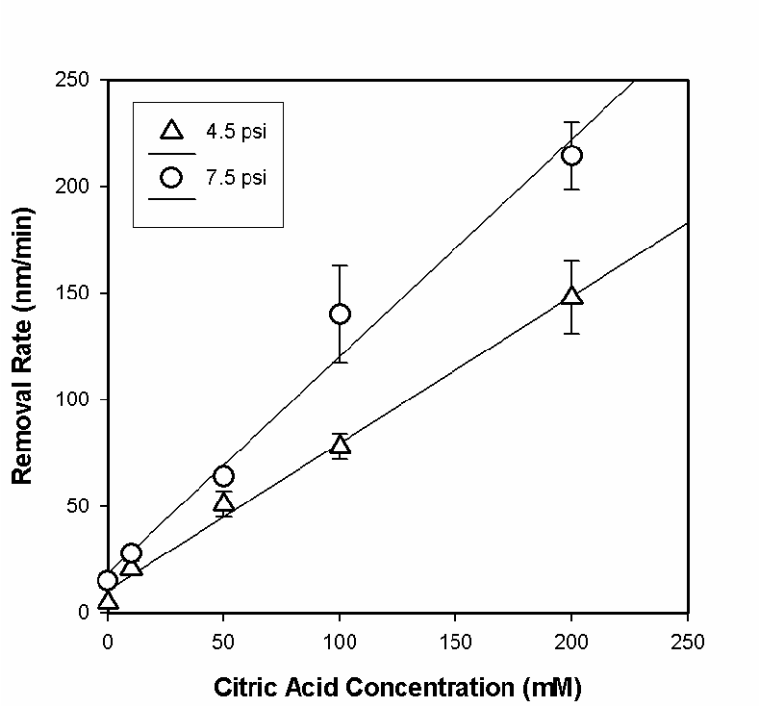

Figure 5-1 Removal rate of copper vs. citric acid concentration in the presence of 5 % hydrogen peroxide and 10 mM BTA at pH 7.

Dissolution / Passivation

First, static etch rate was measured as a function of citric acid concentration in several aqueous media at pH 7. The rate values were taken from the thickness loss of copper after dipping in the test solutions. As shown in Fig. 5-2, the etch rate slightly increases with increasing citric acid content in deionized water. The etching effect is enhanced with the addition of 5 % hydrogen peroxide but shows saturation with an excess amount of citric acid (above 100 mM). It is also shown that the chemical dissolution effect enhanced by the mixture of hydrogen peroxide and citric acid can be completely suppressed by addition of 10 mM BTA due to its inhibitive action.

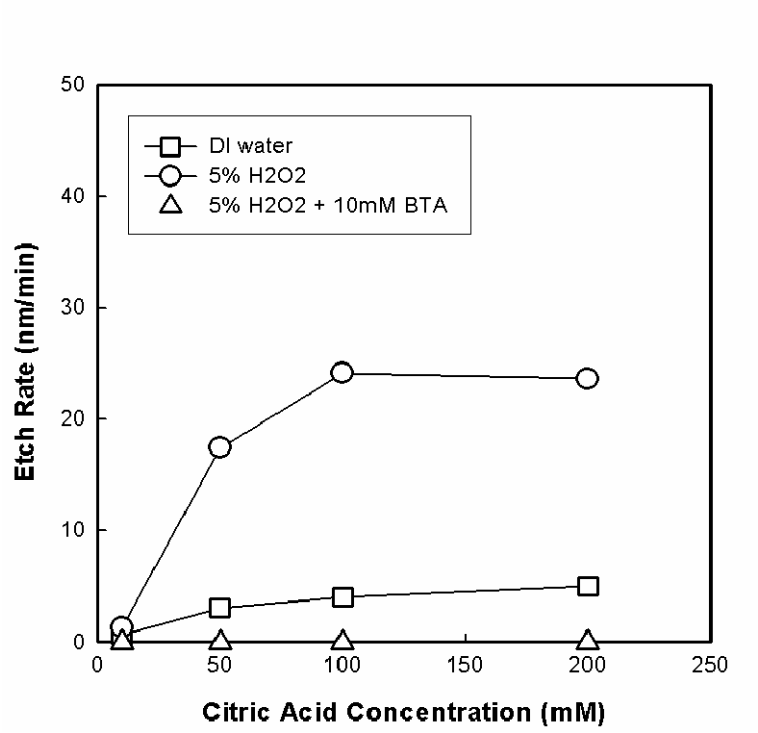

Figure 5-2 Effect of citric acid concentration on copper etch rate in various aqueous media; deionized water (open square), 5 % H_2O_2 (open circle), 5 % H_2O_2 and 10 mM benzotriazole (open triangle) at pH 7.

Potentiodynamic scans of copper were also conducted in several aqueous media. The plots of SCE vs. logarithmic current density are shown in Fig. 5-3. Much higher open-circuit potential of copper is observed in the 5 % hydrogen peroxide solution than that in the 200 mM citric acid solution. Mixed solution of these two agents exhibits both higher open-circuit potential and higher corrosion current density than those in individual ones. Similarly to the static etch rate result, the addition of BTA is also shown to be effective in surface passivation. The values of open-circuit potential and corrosion current density are summarized in Table 1. Dissolution rate of copper was calculated from the current density and compared with the values from thickness loss method. The dissolution rate values taken from the potentiodynamic scans were higher than that from the thickness loss measurements. The limited resolution of thickness measurement by four point probe

method and different time scale of measurements may account for the disagreement. Nevertheless, both results show similar trend in dissolution/passivation behavior with chemistry variations.

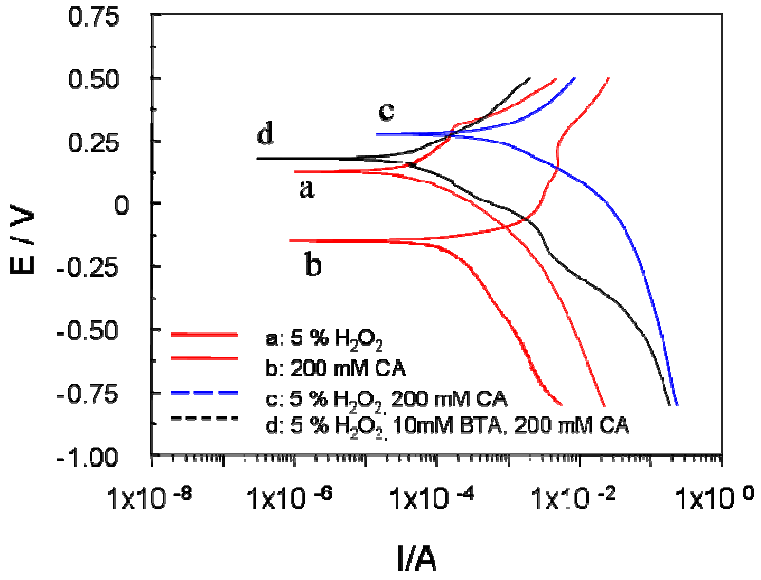

Figure 5-3. Effect of citric acid on polarization curves in various aqueous media at pH 7.

Surface Chemical Composition

X-ray photoelectron spectroscopy (XPS) was used to examine how citric acid influences the chemical composition of the copper surface modified by hydrogen peroxide. Fig. 4a shows the XPS spectra of a copper specimen after dipping in 5% hydrogen peroxide and 100mM citric acid. The $Cu2P_{3/2}$ line and its satellite are observed at 933.6 eV and 943.3 eV with very weak intensity, indicating relatively thin CuO formation on the surface. Cu_2O and $Cu(OH)_2$ are also revealed from O1s binding energy of 530.4 eV and 531.3 eV, respectively. Moreover, C1s of carboxylic acid group (-COOH-) is found at 288 eV, indicating that citric acid complex exists on the surface. To further study the inner layer composition, the specimen was sputtered with Ar+ ions for 12 and 48 seconds.

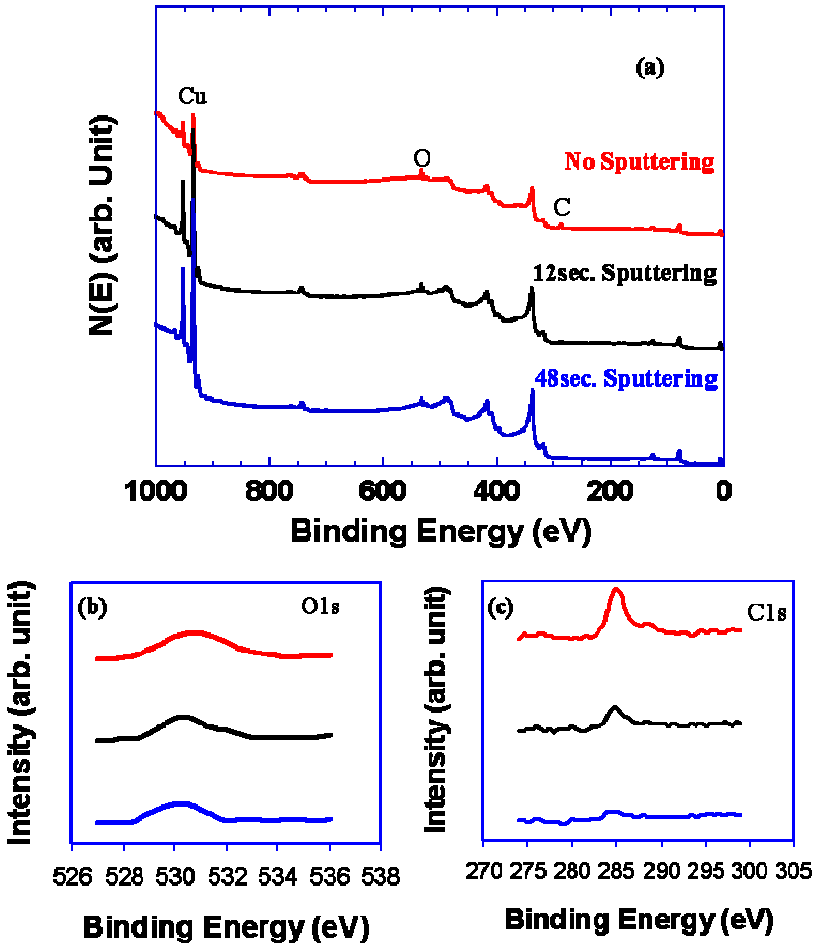

Figure 5-4 (a) The XPS spectra of copper surface treated with 5 % H_2O_2, 10 mM benzotriazole, and 100 mM citric acid at pH 7 with different sputtering time, (b) O1s line, (c) C1s line.

After sputtering for 12 seconds, the carboxylic acid group starts to vanish as shown in Fig 4c. After 48 second-sputtering, the carboxylic acid group is mostly disappeared while Cu_2O is still observed with the same intensity (Fig. 5-4b), indicating that the oxide is the main component of the surface layer.

Reaction Kinetics

An important aspect relevant to the layer formation is the rate at which the particle abrasion takes place, which is generally considered in the range of 10 to 400 milliseconds depending upon the slurry variables [Sin02b]. To study the effect of citric acid on the

dynamic nature of layer growth in the short-time scale, chronoamperometry technique was used. Figure 5-5a shows the transient behavior of surface layer formation on copper in the millisecond range (< 0.07 sec). When only citric acid is used, rate of the layer growth is relatively low. When hydrogen peroxide is added to the citric acid solution, the growth becomes much faster, and the dependence of layer thickness on time is almost linear. The addition of BTA in the mixed solution decreases the growth rate, but the rate is still higher than that in the citric acid solution. The layer growth was also monitored as a function of citric acid concentration in the presence of the peroxide and BTA, which is shown in Fig. 5b. The figure shows that the increase of citric acid concentration enhances the reaction kinetics.

Physical Properties of Surface Modified Surface

The hardness and density of the layer were measured using nanoindentation and XRR, respectively, as a function of citric acid concentration in neutral solutions that contain 5 % hydrogen peroxide and 10 mM BTA. Figure 5-6 shows that the both the hardness and density of the surface layer is significantly decreased by the addition of citric acid in the slurry; approximately 40 % decrease in hardness and 21 % decrease in density with 100 mM of citric acid content.

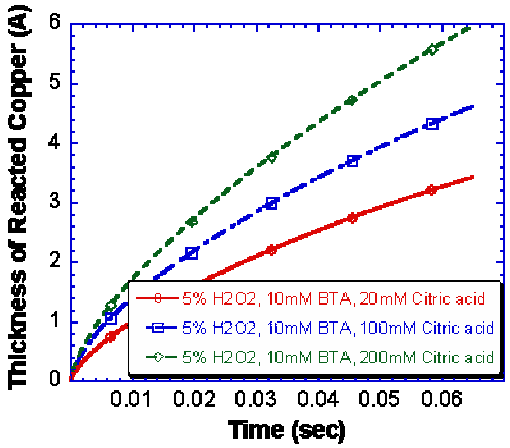

(a)

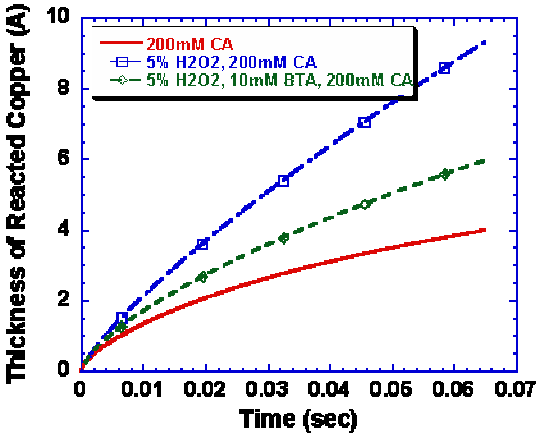

(b)

Figure 5-5 Transient response of layer growth on copper in the millisecond regime (a) effect of citric acid in various media (b) effect of citric acid concentration in the aqueous media that contains 5 % H_2O_2 and 10 mM BTA.

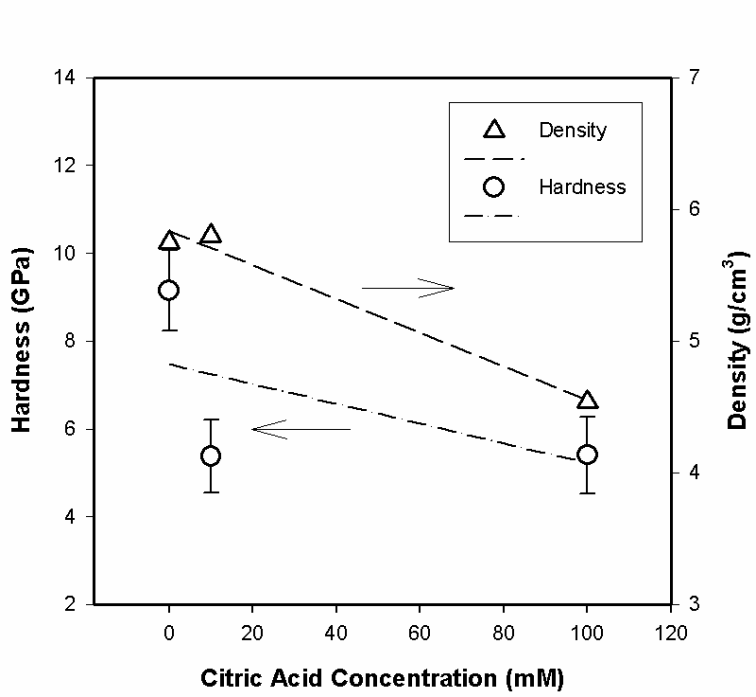

Figure 5-6 Effect of citric acid addition on the hardness and the density of the surface layer; 5 % H_2O_2 and 10 mM benzotriazole at pH 7.

Discussion

Citric acid is a chelating agent with tetra-dentate carboxylic groups that can lose protons and become a citrate ion. Tamilmani et al. [Tam02] suggested that, based on thermodynamic calculations (pH-potential diagrams), presence of the citrate ions in the slurry would tend to chemically dissolve copper through complex formations. According to the pH-potential diagram, doubly charged anionic complex ($Cu(H_{-1}L)^{2-}$, where L = $C_6H_5O_7^{3-}$) is predominant at the neutral pH. Despite the rational identification of stable species under given conditions, only the thermodynamically favorable and predominant species appear on the diagram. Our result of XPS with sputtering, in fact, shows that top surface of the copper specimen treated with the peroxide and citric acid at neutral pH is mainly composed of copper oxide, not the copper-citric acid complex. This implies that the enhanced dissolution effect from the mixture of the peroxide and citric acid in Fig. 5-2

and Fig. 5-3 is attributed to oxide etching, which may take place by two main reactions; oxidation of copper (1), responsible for the oxide formation, followed by complexation (2), responsible for the oxide dissolution.

$$Cu = Cu^{2+} + 2e^{-} \quad (1)$$

$$Cu^{2+} + \text{citrate} = \text{Cu-citrate complex} \quad (2)$$

It is believed that above 100 mM of citric acid the total dissolution rate is limited by the oxidation rate, thus showing the saturation (open circle) in Fig. 5-2. The lower etch rate in deionized water is most likely due to relatively thin-native oxide formation by less oxidizing power of water than that of hydrogen peroxide, which is demonstrated by the potentiodynamic scans (Fig. 5-3). It is noted here that the etching effect by the peroxide and citric acid is efficiently suppressed by the addition of BTA over the entire range of citric acid concentration. Regardless of the minimal etch rate with the BTA addition, however, the removal rate is linearly proportional to the citric acid concentration, as shown in Fig. 5-1. Such a discrepancy clearly indicates that the polishing rate of copper under this condition is fully attributed to chemo-mechanical effects, and the polishing mechanism can be better correlated with the transient electrochemical study.

Figure 5-5 shows that the reaction kinetics in the millisecond regime is indeed influenced by the slurry chemistries. A notable feature in this transient study is that, as shown in Fig. 5-5b, the addition of citric acid in the slurry that contains 5 % hydrogen peroxide and 10 mM BTA enhances the layer growth rate, which is not indicated by the static dissolution/passivation study. In addition, the adsorption of BTA is seen to play a role not only in that it prohibits copper from direct dissolution but also in that the layer growth shows parabolic dependence on time. One may reason that the enhanced reaction

kinetics leads to less dense oxide layer, thus decreasing the layer hardness. This is also confirmed by the results of XRR and nanoindentation. The addition of citric acid does degrade the density and the hardness of the surface layer. Based on these observations, we believe that, using nanoparticle-based slurries, the synergistic mechanical-chemical effect by the addition of citric acid that serves to increase the removal rate is solely attributable to the soft layer formation that allows considerable indentation of nano particles, rather than enhancing solubility of copper. The absence of chelating action of citric acid that leads to enhanced copper dissolution is ascribed to (1) effective passivation by use of neutral slurry and by addition of BTA and (2) relatively small amount of debris generated by nano particles.

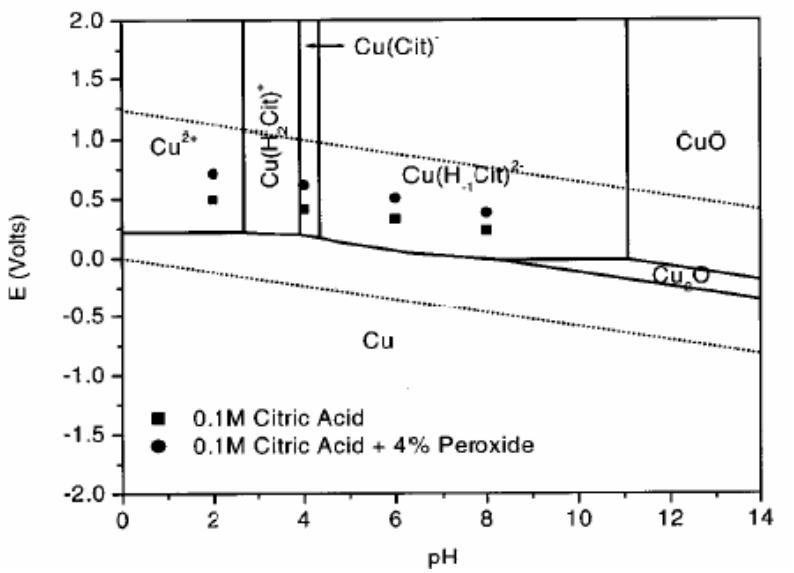

Figure 5-7 Potential-pH diagram for copper-citric acid-water system. Redox potential values of 0.1 M citric acid solution (square) and 0.1 M citric acid with 4 % hydrogen peroxide (circle) are also displayed. ($Cu(H_{-1}L)^{2-}$, where L = $C_6H_5O_7^{3-}$) [Tam03]

Conclusion

We investigated the role of citric acid during copper CMP using silica nanoparticle-based slurries. Linear increase in removal rate was found with an increase of citric acid

content in the presence of hydrogen peroxide and benzotriazole at neutral pH. Static dissolution studies and x-ray photoelectron spectroscopy suggests that copper dissolution is enhanced by the mixture of hydrogen peroxide and citric acid, mostly via oxide dissolution. However, the static etch rate of copper is essentially minimal with addition of BTA but is not well correlated with the removal rate result. In contrast, the transient electrochemical study suggests that reaction kinetics in the millisecond regime is enhanced by citric acid addition even in the presence of BTA, which we believe leads to less dense oxide formation and therefore allows considerable indentation of silica nano particles. This is also confirmed by our results of nanoindentation and XRR, which exhibit that the addition of citric acid in the presence of hydrogen peroxide and benzotriazole significantly decreases the hardness and density of the surface layer. Therefore, using silica nanoparticle-based neutral slurries, the linear increase in removal rate as a function of citric acid concentration can be explained by formation of weakly bonded surface layer, rather than high solubility of copper.

CHAPTER 6
ROLE OF NANOPARTICLE SIZE AND CONCENTRATION

The particle size and concentration play important roles in determining polishing characteristics such as removal rate, surface roughness, etc., and also have been used to help indirectly understand in what manner the material removal occurs during polishing [Sin02]. Nevertheless, experimental results that have been reported with respect to the particle size for polishing of different materials are quite contradicting [Bie99, Mah00]. It has been reported that such contradicting results are also found when the same materials are polished in different particle size ranges such as nano-size particles vs. micron-size particles.

Bielmann et al. [Bie99] studied tungsten CMP using alumina particles ranging 0.3-13 μm and showed that removal rate was inversely dependent of particle size. On the other hand, Bouvet et al. [Bou02] reported that, using sub 100 nm silica particles (12-75 nm), tungsten removal rate was fairly constant with particle size. The conflicting results from different particle size regimes are also seen in oxide CMP. Mahajan et al. [Mah00] used 0.2-1.5 μm silica particles and showed that optimum concentration for high removal rate existed for each particle size, which shifted to a lower concentration with increasing particle size. Such an optimum concentration was not observed when Zhou et al. [Zho02] investigated silica CMP using relatively small silica particles (10-140 nm). Their result suggested that the variation of removal rate with nano-scale particle size was non-linear and the highest removal rate was obtained using 80 nm particle based slurry.

In copper CMP, to our best knowledge, only Lu et al. [Lu03] studied effect of particle size, using silica particles ranging from 50 to 300 nm in hydrogen peroxide and glycine-based acidic slurries. They showed that removal rate increased with a decrease in particle size and suggested that material removal would be controlled by specific surface area of particles. However, as observed in the tungsten and silica CMPs above, use of particles in different size regimes may lead to different polishing phenomena. The study of particle size in copper CMP discretely for the nano-size regime has not yet been conducted.

In this chapter, we investigate the effects of nano-particle size (30-100 nm) and concentration (3-10 wt. %) in copper CMP. The particles are characterized using several techniques. The removal rate and CMP induced-surface roughness are measured with fixed concentration of slurry chemical agents (5 % H_2O_2, 10 mM benzotriazole (BTA) and 100 mM citric acid) at pH 7. In order to understand the wafer-slurry-pad interactions, in situ friction force is measured. Based on these measurements, the role of nano-size silica particles for copper polishing is examined.

Results and Discussion

Particles are characterized using several techniques. Fig. 6-1a shows the size distribution of three different particles (30, 80, 100 nm in approximate mean diameter) obtained by light scattering method, which indicates that each particle size is narrowly distributed. In Fig. 6-1b to c, the images, of particles measured by TEM and SEM are shown, which confirm the particle size and suggest that the particles are quite spherical in shape.

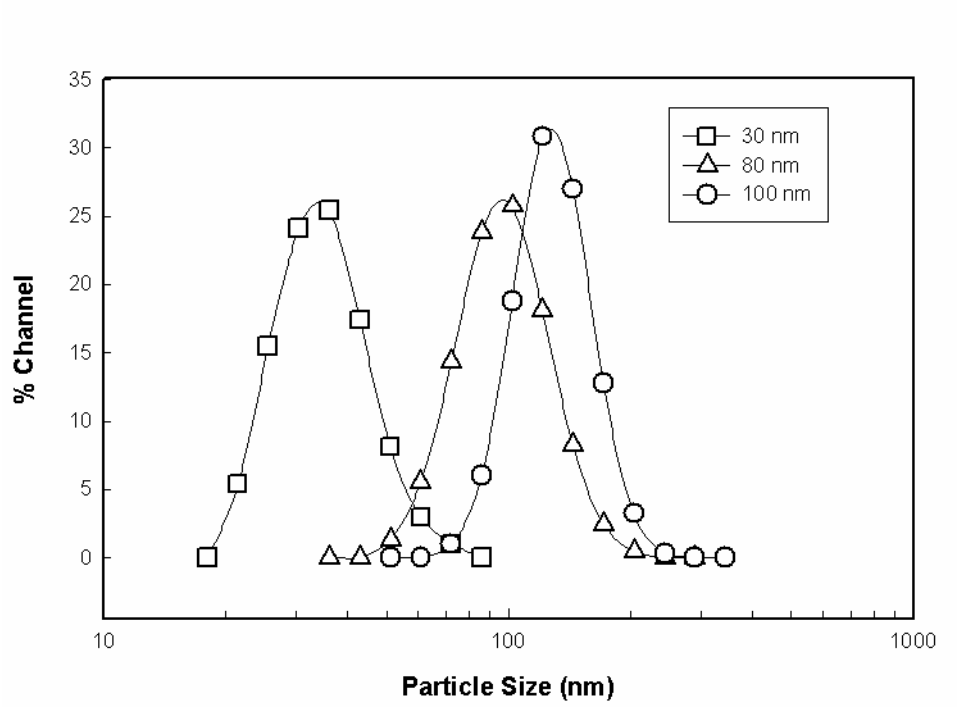

(a)

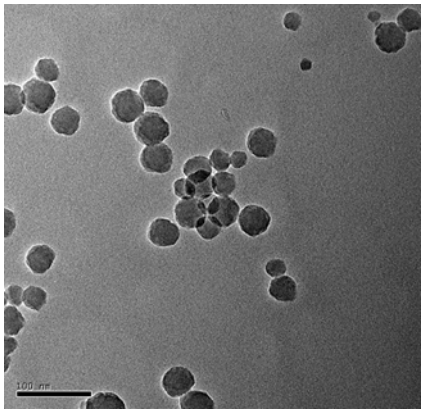

(b)

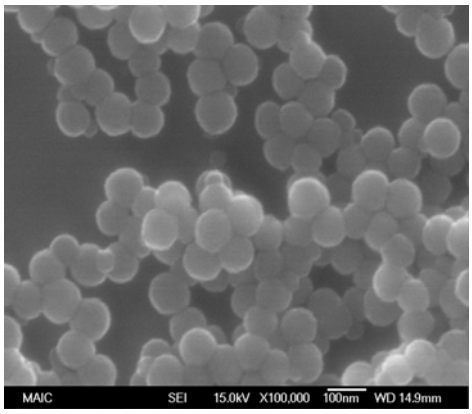

(c)

Figure 6-1 Particle analysis (a) particle size distribution of colloidal silica obtained by light scattering method (b) image of 30 nm colloidal silica obtained by TEM (c) image of 100 nm colloidal silica obtained by SEM.

To study particle size and concentration effects, we selected a specific slurry chemical composition (5 % H_2O_2, 10 mM BTA and 100 mM citric acid at pH 7). Based on our results in chapter four, such a slurry composition exhibits a reasonably high

removal rate without involving chemical dissolution. Figure 6-2 shows the removal rate of copper as function of nanoparticle size (30-100 nm) and concentration (3-10 wt. %). The figure shows the removal rate increases with the increase of both particle size and concentration.

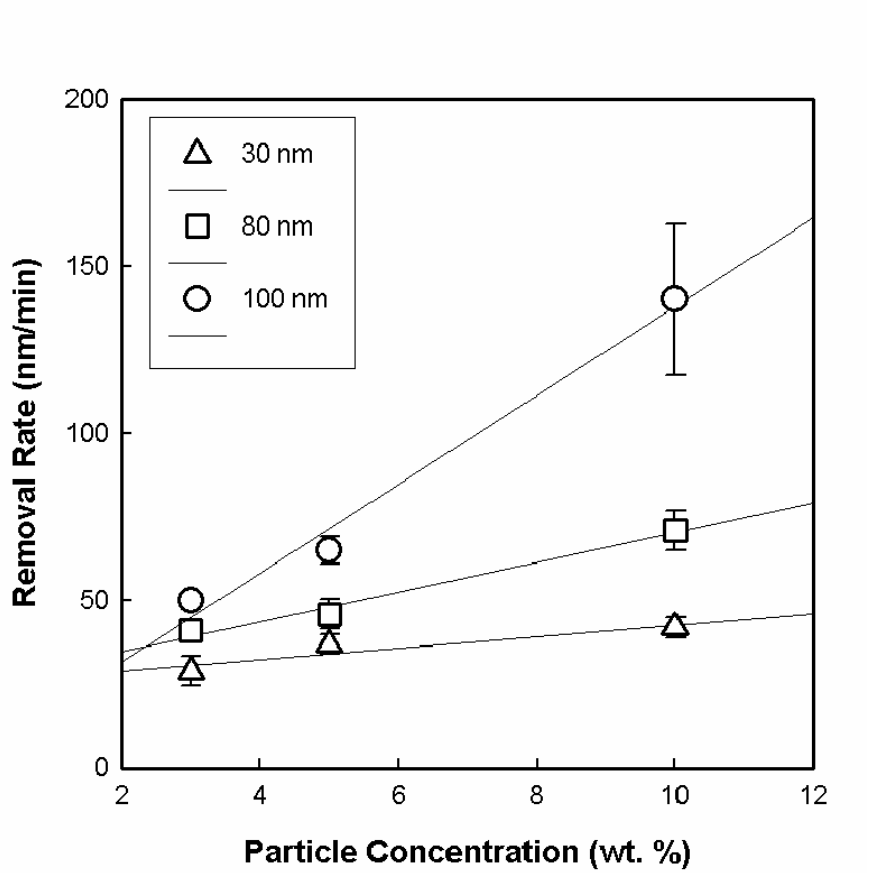

Figure 6-2 Effect of particle size and concentration on removal rate of copper with fixed chemical agents (5 % H_2O_2, 10 mM BTA and 100 mM citric acid) at pH 7 (open circle; 100 nm, open square; 80 nm, open triangle; 30 nm)

The surface topographic image and roughness of the polished samples measured by AFM are shown in Fig. 6-3. As shown in Fig. 6-3a, micro-scratches that are commonly observed after copper CMP process are not exhibited. Figure 6-3b shows that root mean square (RMS) values are very low (> 0.7 nm) and fairly independent of particle size and concentration.

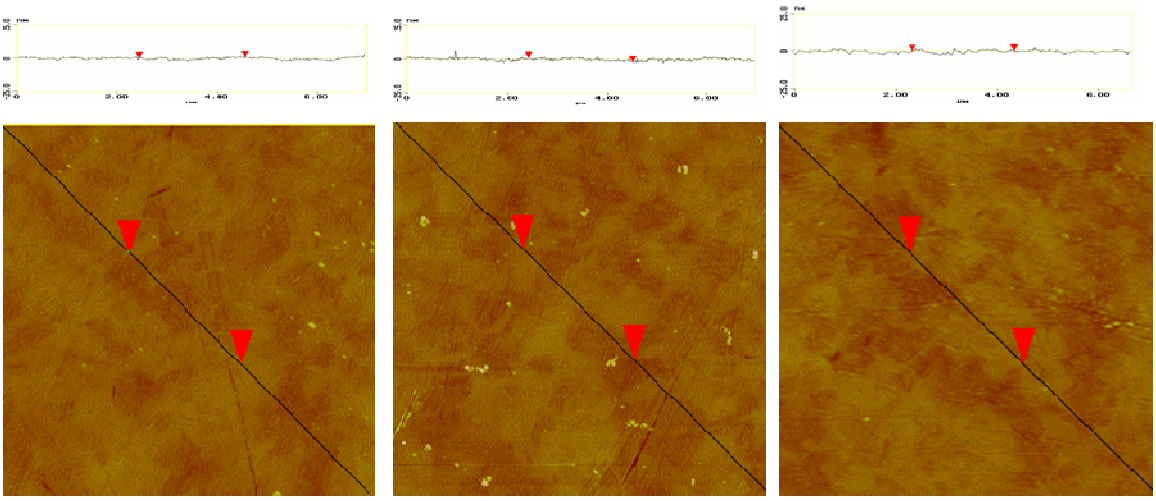

(a) (b) (c)

Figure 6-3 Effect of particle concentration on surface topography after polishing with 100 nm colloidal silica particle (a) 3 wt. % (b) 5 wt. % (c) 10 wt. %

To understand the role of particle size in copper CMP, in situ friction force measurements were conducted on these samples. Figure 6-6 shows the friction force response vs. particle concentration and particle size (30 and 100 nm). Two sets of experiments were conducted: one without citric acid in the slurry (5 % hydrogen peroxide and 10 mM BTA at pH 7, Fig. 6-6a), the other with 100 mM citric acid in the same slurry (Fig. 6-6b). In both cases, friction force increases with increasing particle size and concentration. However, friction force response becomes much more dependent on particle size and increases more rapidly with increasing particle concentration as 100 mM citric acid is added in the polishing slurry (Fig. 6-6b).

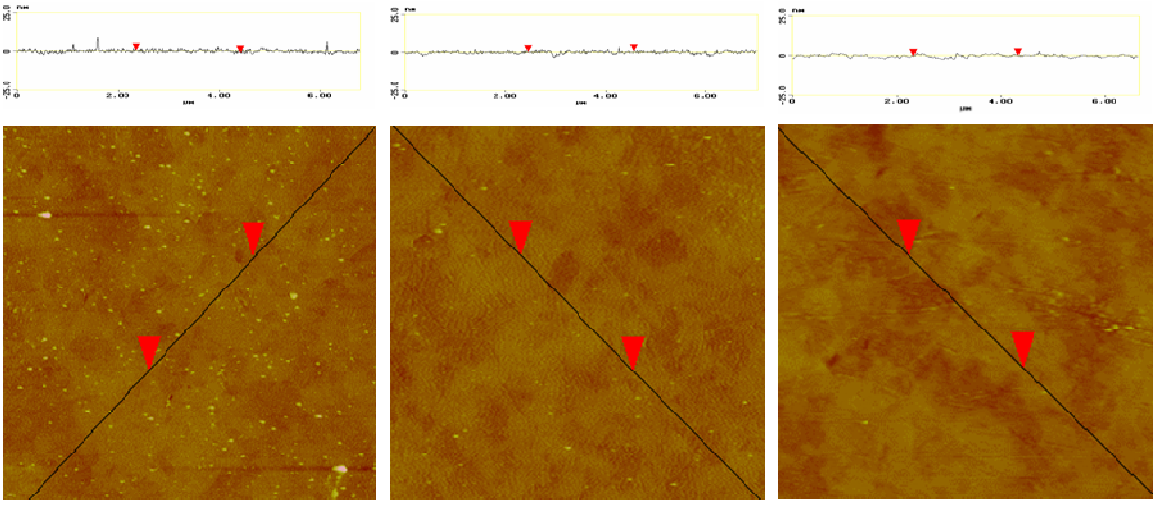

(a) (b) (c)

Figure 6-4 Effect of particle size on surface topography after polishing with 10 wt. % solids loading (a) 30 nm (b) 80 nm (c) 100 nm.

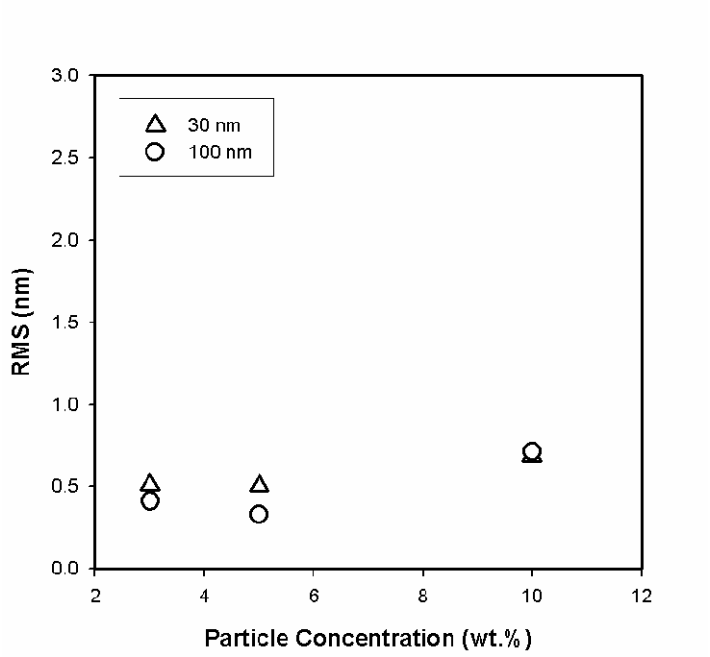

Figure 6-5 Effect of particle size and concentration on surface roughness (RMS) of copper specimen after polishing.

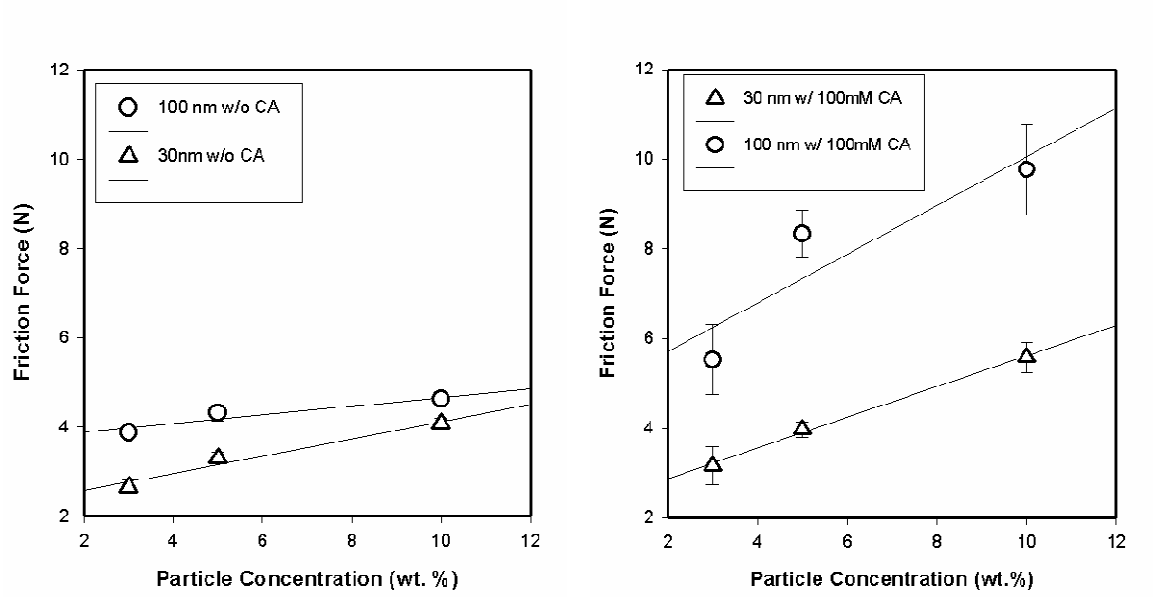

Figure 6-6 Effect of particle size and concentration on friction force during copper polishing (a) without citric acid in the slurry (5% H_2O_2, 10mM BTA at pH 7) (b) with addition of 100mM citric acid.

In contrast to earlier results by Lu et al. [Lu03], the removal rate obtained in this study increases with increasing particle size. It should be noted that, in copper CMP, the nano-particle polishing results are quite different compared to sub-micron size particle polishing in which we observed much high rms values and deeper scratches in chapter four. As shown in Fig. 6-3 and Fig. 6-4, the copper surface polished with nanoparticles does not involve the microscratches and the RMS value is independent of the particle size, which suggest that, due to nanoparticle characteristics of shallow indentation, the material removal occurs without significantly damaging the sub bare copper underneath the chemically modified surface layer.

The slurry chemistry also significantly influences copper surface properties such as dissolution/passivation behavior or surface layer formation mechanism, and consequently influences the polishing characteristics. It is conceivable that the material removal in the work by Lu et al. includes high level of chemical dissolution. The removal rate obtained

without use of abrasives was exceedingly high (> 200 nm/min), which may not be the appropriate slurry environment to study the pure effect of particle size. On the other hand, we earlier showed that the slurry chemical condition selected for this study did not involve chemical dissolution, but rather form a passive surface layer that can be indented and removed by the nanoparticles. Detailed discussion of the removable layer formation is presented in chapter 5.

The friction force result shown in Fig. 6-6 implies that the particle indentation volume plays an important role in material removal. Choi et al. [Cho04] utilized the in situ friction force approach to estimate the fractional surface coverage of particle at the pad-wafer contact area. To minimize the effect of particle indentation on the friction force measurement, the experiments were conducted using soft silica particles (*540 kg/mm^2) and hard sapphire wafer (*2370 kg/mm^2). Their experimental result showed that the friction force increased as the particle size decreased and as the particle concentration increased. The larger friction force responses for the smaller particles were explained by their larger surface area (or larger number of contact). Note that the number of smaller particles is greater than that of bigger particles at the same particle concentration (wt. %). Our measurement result obtained in this study is similar to Choi's result in that the friction force increases as particle concentration increases, but shows disagreement in the particle size effect on the friction force responses. Such conflicting results in the particle size effect on friction force are attributable to the particle indentation on the wafer surface. A proposed schematic of nanoscale particle-copper surface interactions is illustrated in Fig. 6-7. It is believed that the particle indentation is limited within the

* Vicker's hardness [Ric71]

surface layer because of the characteristics of nanoparticles, and the larger particles (100 nm) with larger indentation volume may lead to higher friction force and more efficient material removal.

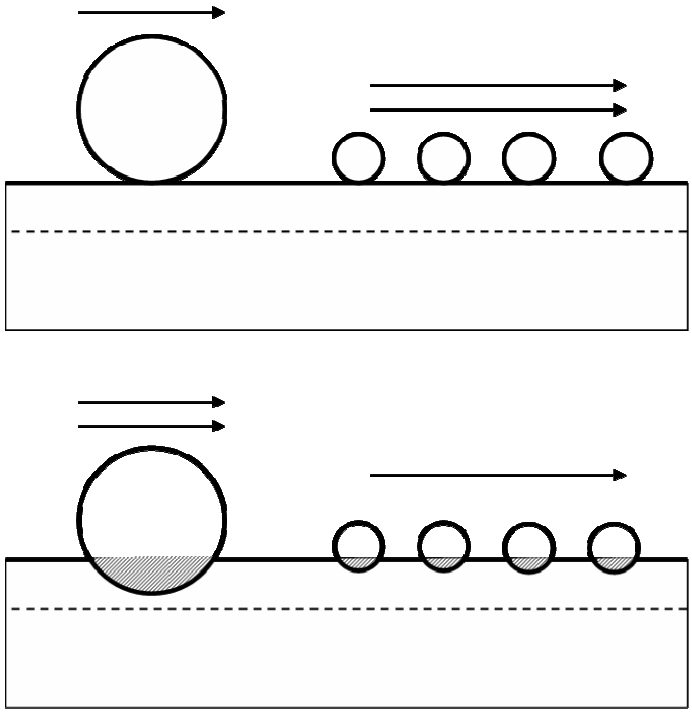

Figure 6-7 Schematic illustration of nanoscale particle-wafer surface interactions. Dashed line shows the boundary of surface layer formed by chemical agents during polishing. The figure shows that the bigger particles (100 nm) can have larger indentation volume on the surface layer which leads to higher friction force and more efficient material removal.

Conclusion

We have investigated the role of particle size below 100 nm in mean diameter during chemical mechanical polishing (CMP) of copper. Our experiment results exhibit following;

1. Copper removal rate increases as the nanoparticle size and concentration increase.

2. Microscratches were not found on surface of nay copper specimen after polishing. The RMS values were very low (< 0.7 nm) and were independent of nanoparticle size and concentration.
3. In situ friction force also increases as the nanoparticle size and concentration increase.

It is believed that, due to the shallow indentation characteristics of the nanoparticles, the material removal occurs within the surface layer formed by chemical additives without severely damaging the sub bare copper. In situ friction force result suggests that the increased copper removal rate with increasing nanoparticle size is attributable to the larger indentation volume.

CHAPTER 7
CONCLUSION

We have investigated copper CMP using nanoparticle-based slurries. With addition of citric acid in the presence of hydrogen peroxide and benzotriazole at pH 7, we obtained moderate removal rates with very low rms values, less than 0.7 nm. Micron-size silica and 200 nm alumina particles were also used as comparison.

1. The hardness and size of the particles can be reduced to lower the penetration depth, thus avoiding damaging effects. However, reducing particle hardness and size without use of synergistic chemistries may lead to much reduced removal rates.

2. The addition of complexing agent, citric acid, in the slurry is critical to the formation of surface layer removable by the colloidal silica nanoparticles.

3. In contrast, larger or harder particles result in greater surface defects suggesting that removal takes place via scratching process.

We propose that citric acid softens the surface layer formed by hydrogen peroxide and benzotriazole, and results in larger indentation depth of nano-size silica particles, thus increasing the removal rate. Combined mechanical-chemical effects are needed to achieve low-defectivity polishing of copper.

We investigated the role of citric acid during copper CMP using silica nanoparticle-based slurries. Linear increase in removal rate was found with an increase of citric acid content in the presence of hydrogen peroxide and benzotriazole at neutral pH. Static dissolution studies and x-ray photoelectron spectroscopy suggests that copper dissolution is enhanced by the mixture of hydrogen peroxide and citric acid, mostly via oxide dissolution. However, the static etch rate of copper is essentially minimal with addition of

BTA but is not well correlated with the removal rate result. In contrast, the transient electrochemical study suggests that reaction kinetics in the millisecond regime is enhanced by citric acid addition even in the presence of BTA, which we believe leads to less dense oxide formation and therefore allows considerable indentation of silica nano particles. This is also confirmed by our results of nanoindentation and XRR, which exhibit that the addition of citric acid in the presence of hydrogen peroxide and benzotriazole significantly decreases the hardness and density of the surface layer. Therefore, using silica nanoparticle-based neutral slurries, the linear increase in removal rate as a function of citric acid concentration can be explained by formation of weakly bonded surface layer, rather than high solubility of copper.

We have investigated the role of particle size below 100 nm in mean diameter during chemical mechanical polishing (CMP) of copper. Our experiment results exhibit following;

1. Copper removal rate increases as the nanoparticle size and concentration increase.
2. Microscratches were not found on surface of nay copper specimen after polishing. The RMS values were very low (< 0.7 nm) and were independent of nanoparticle size and concentration.
3. In situ friction force also increases as the nanoparticle size and concentration increase.

It is believed that, due to the shallow indentation characteristics of the nanoparticles, the material removal occurs within the surface layer formed by chemical additives without severely damaging the sub bare copper. In situ friction force result suggests that the increased copper removal rate with increasing nanoparticle size is attributable to the larger indentation volume.

LIST OF REFERENCES

[Aks02] S. Aksu and F.M. Doyle, *J. Electrochem. Soc*., 149, 6 (2002) p. G352

[Aks03] S. Aksu, L. Wang, and F.M. Doyle, *J. Electrochem. Soc*., 150, 11 (2003) p. G718

[Bas00] G.B. Basim, J.J. Adler, U. Mahajan, R.K. Singh, and B.M. Moudgil, *J. Electrochem. Soc.*, 147, 9, (2000) p. 3523

[Bas03] G.B. Basim, I.U. Vakarelski, and B.M. Moudgil, *J. of Colloid. And Interface. Sci.*, 263 (2003) p. 506

[Bie99] M. Bielmann, U. Mahajan, and R.K. Singh, *Electrochem. Solid-State Lett.*, 2, 8 (1999) p. 401

[Bou02] D. Bouvet, P. Beaud, P. Fazan, R. Sanjines, and E. Jacquinot, *J. Vac. Sci. Technol. B*, 20, 4 (2002) p. 1556

[Bro81] N.J. Brown, P.C. Baker and R.T. Maney, *Proc. SPIE*, 306 (1981) p. 42

[Bru92] C.R. Brundle, C.A. Evans Jr. and S. Wilson, "*Encyclopedia for Materials Analysis-Surfaces, Interfaces, Thin Films*," Elsevior (1992)

[Cha03] Chang, J. Shieh, B. Dai, M. Feng, Y. Li, C.H. Shih, M.H. Tsai, S.L. Shue, R.S. Liang, and Y. Wang, *Electrochem. and Solid-State Lett.*, 6, 5 (2003) p. G72

[Che04] J. Chen and W. Tsai, *Mater. Chem. Phys.,* 87, 2-3 (2004) p. 387

[Cho04] W. Choi, S. Lee, J.T. Abiade, and R.K. Singh, *J. Electrochem. Soc*. 151, 5 (2004) p. G368

[Coo90] L.M. Cook, *J. Non-Cryst. Solids*, 120 (1990) p. 152

[Du04] T. Du, A. Vijayakumar, and V. Desai, *Electrochimica Acta*, 49, 25 (2004) p. 4505

[Gre66] J.A. Greenwood and J.B. Williamson, *Proc. Royal Soc. A*, 395 (1966) p. 300

[Gre67] J.A. Greenwood, *J. Lubrication Tech.* Jan. (1967) p. 81

[Intel] www.intel.com

[Kau91] F.B. Kaufmann, D.B. Thompson, R.E. Broadie, M.A. Jaso, W.L. Githrie, D.J. Pearson, and M.B. Small, *J. Electochem. Soc.* 138 (1991) p. 3460

[Kne97] E.A. Kneer, C. Raghunath, J.S. Jeon, and S. Raghavan, *J. Electrochem. Soc.*, 144 (1997) p. 1934

[Kon03] S. Kondo, B.U. Yoon, S. Tokitoh, K. Misawa, S. Sone, H.J. Shin, N. Ohashi and N. Kobayashi, *IEEE Technical Digest - International Electron Devices Meeting,* (2003) p. 151

[Lee03] S. Lee, dissertation, *"Characterization of Chemical Interactions during Chemical Mechanical Polishing of Copper,"* University of Florida (2003)

[Lu03] Z. Lu, S. Lee, S.V. Babu, and E. Matijevic, *J. Colloid and Interface Sci.* 261 (2003) p. 55

[Mah99a] U. Mahajan, M. Bielmann, and R.K. Singh, *Electrochem. and Solid-State Lett.* 2, 1 (1999) p. 46

[Mah99b] U. Mahajan, M. Bielmann, and R.K. Singh, *Electrochem. and Solid-State Lett.* 2, 2 (1999) p. 80

[Mah00] U. Mahajan, M. Bielmann, and R.K. Singh, *Materials Research Society Symposium*, 566 (2000) p. 27

[Mur00] S.P. Murarka, I.V. Verner, and R.J. Gutmann, "*Copper-fundamental mechanisms for microelectronic applications*" (2000) John Wiley, New York

[Oer85] G. Oertel, *"Polyurethane Handbook,"* Macmillan, New York, 1985

[Pad03] D. Padhi, J. Yahalom, S. Gandikota, and G. Dixit, *J. of Electrochem. Soc.*, 150, 1 (2003) p. G10S

[Pou74] M. Pourbaix, "*Atlas of Electrochemical Equilibria in Aqueous Solution*", NACE, Houston, TX (1974)

[Pre27] F. Preston, *J. Soc. Glass Technol.*, 112, (1927) p. 14

[Qin04] K. Qin, B. Moudgil, and C. Park, *Thin Solid Films*, 446, 2 (2004) p. 277

[Ric71] R. W. Rice, in *Materials Science Research, Vol. 5: Ceramics in Severe Environments* (1971) p. 195, edited by W. W. Kriegel and H. Palmour III, Plenum, New York

[Rya05] J.G. Ryan, R.M. Geffken, N.R. Poulin, and J.R. Paraszczak, *IBM J. Res. Dev.*, 39, 4 (1995) p. 371

[Sho00] L. Shon-Roy, *"CMP: Market trends and technology," Solid State Technology,* 43, 6 (2000) p. 67

[Sin02a] R.K. Singh and R. Bajaj, *Material Research Society Bulletin*, 27 (2002) p. 743

[Sin02b] R.K. Singh, S. Lee, K. Choi, D.B. Basim, W. Choi, Z. Chen, and B.M. Moudgil, *Material Research Society Bulletin*, 27 (2002) p. 752

[Sin03] R.K. Singh and S. Lee, 8th International Proceedings, *Chemical Mechanical Planarization for ULSI Interconnection Conference (CMP-IMIC)*, Feb. (2003) p. 128

[Ste97] J. M. Steigerwald, S.P. Murarka, and R.J. Gutmann, "*Chemical Mechanical Planarization of Microelectronic Materials*" (1997) John Wiley & Sons, New York

[Ste99] D.J. Stein, D.L. Hetherington, and J.L. Cecchi, *J. Electrochem. Soc.,* 146 (1999) p. 1934

[Tam02] S. Tamilmani, W. Huang, S. Raghavan, and R. Small, *J. Electrochem. Soc.,* 149, 12 (2002) p. G638

[Tic99] J. Ticky, J.A. Levert, L. Shan, and S. Danyluk, *J. Electrochem. Soc.*, 146 (1999) p. 1523

[Yu93] Y. Yu, C.C. Yu, and M. Orlowski, *IEEE IEDM*, 865, 65 (1993) p. 35.4.1

[Wan01] S. Wang, G. Grover, C. Baker, J. Chamberlain, and C. Yu, *Solid State Technology*, September (2001) p. S9

[Zha02] Y. Zhao and L. Chang, *Wear*, 252 (2002) p. 220

[Zho02] C. Zhou, L. Shan, J.R. Hight, S. Danyluk, S.H. Ng, and A.J. Paszkowski, *Tribology Transactions*, 45, 2 (2002) p. 232

BIOGRAPHICAL SKETCH

Su-Ho Jung was born on May 9, 1973, in Seoul, South Korea. He graduated in 1999 with a bachelor's degree in materials science and engineering from Kangwon National University in Chunchon, South Korea. While he was pursuing the bachelor's degree, he served in Korean National Army for a year and a half, and also spent two semesters at Cornell University, Ithaca, New York, attending an intensive English program. He started his graduate study in the department of materials science and engineering at the University of Florida, Gainesville, Florida, in fall 1999. His master's research was supported by the Department of Energy and focused on the oxide ionic conductors for the fuel cell application under the advisory of Professor Eric Wachsman. He graduated in fall 2001 with a master's degree and a thesis titled "Cubic Bismuth Oxides and Their Application in Low Temperature Solid Oxide Fuel Cells." In spring 2002, he joined the Professor Rajiv Singh's research group for his Ph.D. work and started an investigation mainly on understanding the copper chemical-mechanical polishing (CMP) mechanism towards low-defect purposes. His work also ranged over versatile subjects such as compound semiconductor CMP and shallow trench isolation CMP. He graduated from the University of Florida with a doctoral degree in materials science and engineering in May 2005.